Precision Engineering 76 (2022) 29–51

Contents lists available at ScienceDirect

Precision Engineering

journal homepage: www.elsevier.com/locate/precision

Injection molding of high-precision optical lenses: A review

Carina Peixoto [a], Pablo T. Valentim [b], Patrícia C. Sousa [b], Diana Dias [a], Cátia Araújo [a], Diogo Pereira [a], Catarina F. Machado [c], Antonio J. Pontes [c], Hélio Santos [d], Sílvia Cruz [a,*]

[a] PIEP – Innovation in Polymer Engineering, University of Minho, 4800-058, Guimarães, Portugal
[b] INL - International Iberian Nanotechnology Laboratory, 4715 330, Braga, Portugal
[c] IPC – Institute of Polymers and Composites, Department of Polymer Engineering, University of Minho, 4800-058, Guimarães, Portugal
[d] InovePlastika, S.A, 4755-521, Barcelos, Portugal

ARTICLE INFO

Keywords:
Injection molding
Optics
Residual stress
Anti-reflective coatings
Micro and nanostructures

ABSTRACT

Injection molding (IM) is the most efficient mass production technology for manufacturing polymers in complex and detailed geometries with high precision. Although, with the demanding requirements for the optical components, the manufacturing process continues to be a challenge. The majority of optical components require high optical quality with low residual stress, high replication degree, and precisely controlled surface contours, which require a high control of the processing parameters and high-precision optical mold inserts. The main scope of this review is to describe recent progress in the IM, in particular, in the production of high-precision optical lenses. Thereby, an overview of the influence of process parameters, the emerging technologies able to improve the quality of molded components, and the fabrication technologies to produce optical inserts are provided. Furthermore, this review also reports the enhancement of optical performance by using optical coatings. Anti-reflective (AR) coatings, their fabrication techniques, as well as the methodologies typically employed for characterization are also addressed.

1. Introduction

In recent years, polymers have undergone great growth in the production of optical components, in special optical lenses such as Fresnel lenses, freeform lenses, aspheric lenses, microlens, or microlenses arrays, and diffractive optical elements, thus far manufactured from glass. Optical polymers allow complex optical designs with several surfaces and various assembly features, previously limited to the demand and high-cost manufacturing processes of glass. These products have been used widely in various fields, such as automotive [1], lighting [2], photovoltaic [3], electronics [4–7], ophthalmology [8], and medical [9].

In the development of optical lenses, the surface quality, curvature, and surface optical design are extremely important to describe their optical performance. Depending on the purpose, different lenses may be used, such as simple spherical lenses and aspherical lenses, as well as freeform and microstructured lenses. However, not only the geometry affects the performance and functionality, but the combination of material, manufacturing process, process condition, and mold, may also lead to different optical functionality [10]. Manufacturing techniques such as IM, injection compression molding (ICM), and microinjection molding (μ IM) have been increasingly used in the production of optical components, allowing high production rates, low cost, and automation, which helps the mass production of these components [11]. These techniques may reproduce complex geometries and microstructures, with optical properties comparable to glass with the advantage of high reproducibility [10].

The most common polymers used in the production of optical components are Poly(methyl methacrylate) (PMMA) best known for acrylic [12], polycarbonate (PC) [13], cyclic olefin copolymer (COC) [14], and cyclic olefin polymer (COP) [15], which provide good technical properties regarding internal stresses, low water absorption, and optimized weather resistance. In combination with microstructured features, their optical properties may be enhanced and become similar to optical glass [16]. Furthermore, additional functions can be conferred by depositing coatings on a polymer optical lens after IM, which enables the

* Corresponding author. PIEP- Innovation in Polymers Engineering, Universidade do Minho, 4800-085, Guimarães, Portugal.
E-mail addresses: carina.peixoto@piep.pt (C. Peixoto), pablo.valentim@inl.int (P.T. Valentim), patricia.sousa@inl.int (P.C. Sousa), diana.dia@piep.pt (D. Dias), catia.araujo@piep.pt (C. Araújo), diogo.pereira@piep.pt (D. Pereira), catarinafmachado@dep.uminho.pt (C.F. Machado), pontes@dep.uminho.pt (A.J. Pontes), helio.santos@inoveplastika.pt (H. Santos), silvia.cruz@piep.pt (S. Cruz).

https://doi.org/10.1016/j.precisioneng.2022.02.002
Received 13 September 2021; Received in revised form 7 December 2021; Accepted 1 February 2022
Available online 18 February 2022

enhancement of optical and mechanical performance. In the literature, different coatings have been reported, such as AR coating [17,18] to reduce reflection and improve the lens efficiency, scratch-proof coatings [19] for increased lens durability, anti-fogging coatings [20], and dielectric mirror coatings.

In general, optical lenses need precisely controlled surface contours to realize their optical design, high accuracy (a few microns or less), a surface roughness close to 10 nm, and low birefringence [21]. However, the IM is the main cause of the increase of birefringence and form deviations, due to flow-induced residual stress attributed to molecular orientation during the filling stage, and thermal residual stress due to shrinkage during the cooling stage. In this way, process conditions have a significant effect on the molded lenses quality [22]. The manufacturing of optical components emerges as a great challenge, in many ways, in machine technology, fabrication technologies for optical mold insert as well as in process control. With the development of material science and tooling technology, molded lenses quality may be significantly improved. Even though, the production of optical lenses with microstructures and other geometric details is still not matured and optimized at the industry level. To obtain the exact reproduction of microstructures, the process needs to be optimized concerning the process parameters, which result in small process windows.

It has been demonstrated in the literature, that molded optical parts can achieve well-controlled surface contours and reduced residual stress in the final part by using an appropriate mold and inserts, as well as through process optimization [23–25]. Recent research has been carried out on the analysis and numerical simulations of optical performance [26–30]. In this review, is present the work accomplished so far in the development of optical lenses produced by IM and its variants. Optical polymers and their most important properties, the influence of process parameters as well as the technologies that allow the improvement of optical quality and replication, such as the use of dynamic mold temperature control and vacuum venting are presented. The review also highlights a brief overview of AR coatings on polymer lenses to improve optical performance. Finally, the fabrication technologies for optical mold inserts and the current challenges in the field are discussed.

2. Stress birefringence theory

Stress-induced birefringence is a typical phenomenon inevitable in polymer optical components. As a result of residual stress inside the molded component, a straightening and disentanglement of the molecular chains occur, changing the optical properties in the direction of the stress, which results in an anisotropic material [31]. The refractive index, which represents the ratio of the velocity of light in a vacuum to the velocity of light in a material, varies as a function of stress. Due to the anisotropic property, the refractive index is divided in two directions in a plane and is refracted into two different rays, i.e. ordinary ray and extraordinary ray, and their polarizations are orthogonal [32]. This phenomenon is namely birefringence or double refraction (Δn) and Fig. 1 schematizes the mechanism.

The relation between these parameters, which describes the dependence of the stress and the refractive index, is expressed by Eqs. (1)–(3). It was reported, for a linearly elastic material, a change in refractive index was linearly proportional to the load, and thus to stresses or strains [33].

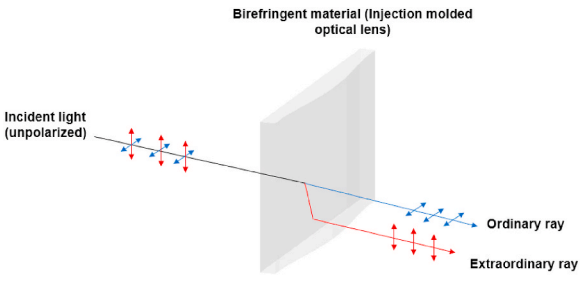

Fig. 1. Schematic illustration of birefringence in an injection molded optical lens.

$$n_1 - n_2 = C(\sigma_1 - \sigma_2) \tag{1}$$

$$n_2 - n_3 = C(\sigma_2 - \sigma_3) \tag{2}$$

$$n_3 - n_1 = C(\sigma_3 - \sigma_1) \tag{3}$$

where σ_1, σ_2, and σ_3 are the principal stresses and n_1, n_2, and n_3 are principal refractive indices at respective principal stress directions. The value of C is a constant, named as stress-optic coefficient or photoelastic coefficient. This parameter is expressed in Brewster (1 Brewster $= 10^{-12}m^2/N = 10^{-13}cm^2/dyn$). In the case of the plane, σ_3 is zero and results:

$$\Delta n = C(\sigma_1 - \sigma_2) \tag{4}$$

where Δn is the birefringence. This equation is known as stress-optic or Brewster law and gives the relationship between the birefringence and residual stress for polymeric materials under stress. The phase difference between the two light rays traveling through the material with thickness, t, at different velocities is known as optical retardation, δ, and is given in nanometers, by Eq. (5). Different stress-optic coefficients result in different induced retardance across the object. According to Eq. (6), higher stress-optic coefficients result in higher retardance [31].

$$\delta = \Delta n \times t \tag{5}$$

$$\delta = C(\sigma_1 - \sigma_2) \times t \tag{6}$$

The isochromatic fringe order, N, can be determined by Eq. (7).

$$N = \frac{\delta}{\lambda} \tag{7}$$

where λ is the wavelength of the incident light. Large fringe orders, or a large number of fringes, indicate regions of high stress. Common and simple equipment used to analyze stress birefringence is a polariscope. The polariscope enables the measurement of the retardation along the ray path and has been used for quality control lens manufacturing processes to identify defects and stress distribution [31]. Fig. 2 shows some examples of the distribution of stress birefringence in optical components. For instance, Fig. 2 (a) shows the residual stress distribution of two different polymers, with different values of stress-optic coefficient.

3. Applications

As previously referred polymer optical lenses may be found in countless fields, from applications with high-precision and tight requirements to more simple geometries that are cost-effective. Nowadays, the optical lenses used in phones cameras, digital cameras, or security cameras are the most know applications and represent a high demand in the optical industry since the 80s [16] and, are mainly used aspherical lenses [4,5].

More recently, in the automobile field, microlenses arrays have been largely used in laser systems and sensors, such as LiDAR systems [1]. As a result of the development of self-driving vehicles, the production of these lenses is expected to grow in the coming years. The microlenses arrays have a microstructured surface and high-precision is required. Typically, this microstructured surface is used to homogenize light paths and to guide the beams into the laser systems. Fresnel lenses are also applied in the automotive industry as lighting for light-emitting diodes (LEDs) [37]. They have a microstructured surface with concentric grooves, which enable enhanced light gathering. Additionally, the Fresnel lenses are widely applied in the photovoltaic industry, for solar

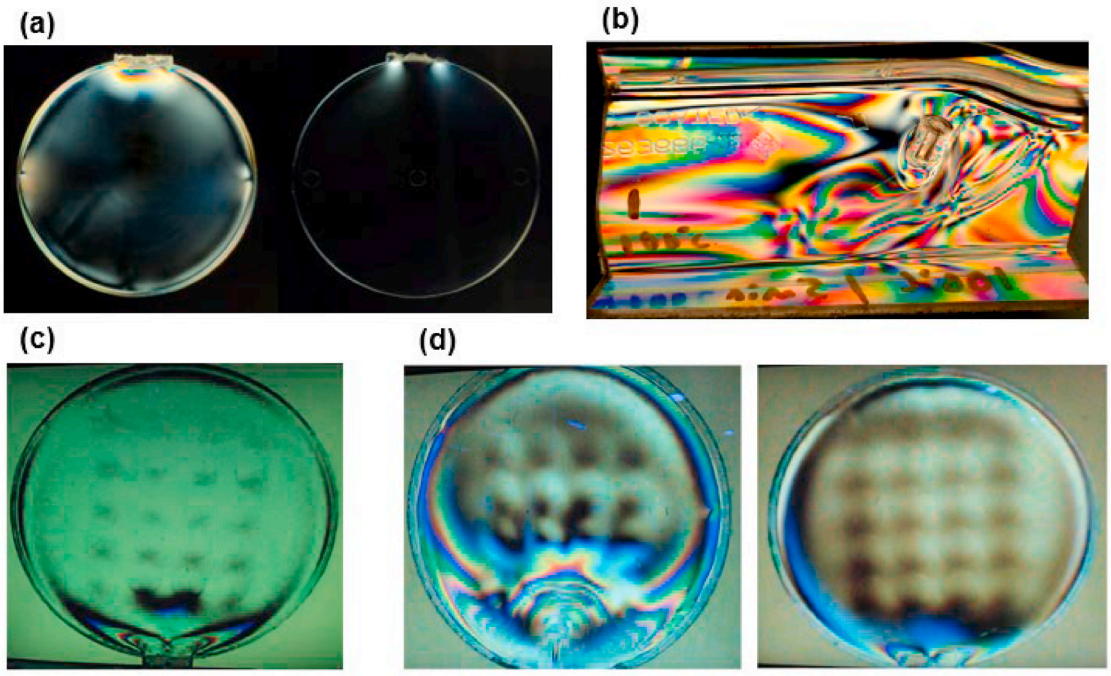

Fig. 2. Examples of photoelasticity analysis: (a) high residual stress of PC optical lenses (Panlite AD5503, Teijin®) (left); and low residual stress of PMMA optical lenses (Plexiglas POQ62, Rhm) (right), analysis through a plane polariscope; (b) plastic cover lens under polarized light. Reprinted with permission from Ref. [34]. Copyright © 2021, Elsevier; (c) injection molded microlens array. Reprinted with permission from Ref. [35]. Copyright © 2021, Elsevier; (d)reduction of residual stress in microlens arrays through optimization of process parameters. Reprinted with permission from Ref. [36]. Copyright © 2021, Elsevier.

concentrator applications [2]. Freeform lenses are mostly applied in illumination, such as LEDs [6], and represent a high-volume application in the optical industry. However, Illumination applications usually need high-volume manufacturing at moderate or very low costs. Hence, this represents a challenge since it is necessary to obtain low contour errors and low surface roughness at limited costs [16,38].

In the medical field, optical lenses also play an important role, as they are essential for imaging processes sensors, medical systems, and lighting devices, for instance, endoscopic imaging systems [9,39]. Furthermore, in the ophthalmology field, eyewear and eye contact lenses are examples of the application of polymer optics as well [5].

Furthermore, functional coatings are widely applied in the optics industry and polymer optical lenses are examples of it, since they may help to overcome some limitations of the polymer optical lenses. They may be used for countless ends, such as thermal control in glazing, impact and scratch resistance, and increased transmission. AR coatings are the most applied since they may eliminate unwanted surface reflections and increase light transmission. In the same way that optical lenses, AR coatings are applied in electronic, photovoltaic solar cells, sensors, such as in lenses applied in automobile industries, camera lenses, and obviously, ophthalmic lenses to reduce reflectance, glare, and enhance light transmittance [40]. Other coatings are applied on the polymer surface that may be combined, or not, with AR coatings, such as anti-scratch coatings, which are essential to improve the mechanical behavior of the PC lenses widely used in eyewear applications [41]. The self-cleaning or superhydrophobic coatings are also broadly used in optical lenses used in outdoor areas, such as outdoor lighting. Although, they are also used in solar photovoltaic panels, optical windows, and windshields [42,43].

In all these fields, it is important to highlight that the adhesion between the polymer surface and the coating is crucial to create an efficient system [44], with chemistry playing an important role in controlling superficial bonding, and these remaining a challenge. However, by modifying or creating new functional groups on the surface of the polymers, or by changing their roughness, it is possible to change the interactions between the substrate and the coating, and consequently, increase their adhesion to other materials [45]. For instance, magnetron sputtering processes for deposition of optical coatings have demonstrated outstanding reliability for the fabrication of complex coating systems such as optical filters for fluorescence spectroscopy and space applications [46,47] or chirped mirrors for ultrashort pulse lasers [48]. In addition to filters, the applications also include optoelectronic devices, ultrasensitive bio-or chemical sensors, absorption enhancement in solar cells, security devices, tunable filters, and display components.

4. Optical polymers

Optical glass has been conventionally used since it is considered as the most reliable material, and is used in lenses for which high stability is required. However, it is not suitable for mass production, due to high cost and difficult precision manufacturing. Thus, in the last years, optical polymers have become great substitutes for optical glass. These materials appear as an extremely promising alternative due to the high impact resistance, low price, lightweight, which may significantly reduce the weight of the complete system, and due to the optical properties similar to glass. In the development of optical lenses, the main requirements are: i) high dimensions stability of the component when is subjected to temperature, pressure variations, or humidity; ii) high geometric accuracy; iii) high light transmittance at specific wavelengths; and iv) low birefringence, which is directly related to optical distortion and can cause light deviation. In the past years, polymers have been developed to answer these requirements. Typically, in the production of optical components, amorphous thermoplastics are used. In the literature, the most reported polymers are PMMA, PC, COC such as TOPAS® manufactured by TOPAS Advanced Polymers, and COP such as ZEONEX® and ZEONOR® manufactured by ZEON Chemicals. With less common use are the Polyetherimide (PEI), commercially named ULTEM®, or polyesters, O-OPET, like OKP4 and OKP4HT.

The refractive index is also an important property in optical polymers. Normally, an optical polymer shows a refractive index between

1.4 and 1.7. The Abbe number is associated with this property and describes how the wavelength is dependent on the refractive index. Higher values of refractive index result in smaller Abbe number, and consequently larger wavelength dispersibility [16]. The main physical and optical properties of these polymers and optical glass are shown in Table 1.

The behavior of polymers during the IM process, the replication achieved, and even the amount of residual stress and warpage, are mainly caused by the rheologic properties and pressure-volume-Temperature (PVT) behavior of each polymer. To better understand, Fig. 3 shows the representative plot of (a) viscosity versus shear rate for the recommended process temperatures and (b) PVT plot for the main optical polymer previously referenced in Table 1.

Despite all the advantages that optical polymers have and their enormous potential, some limitations, which may affect the quality requirements for the optical components, should be considered. The refractive index change with temperature restricts the temperature operation range and application of the polymer in optical systems subject to extreme changes in temperature [51]. Compared with glass, polymers have a lower transition temperature, a higher coefficient of linear expansion, about an order of magnitude higher, and higher water absorption [52]. Among optical polymers shown, the COP, COC, and PC are more suitable in applications exposed to higher temperatures without the risk of deformation, because they have a higher value T_g of than the remaining. Typically, PMMA absorbs approximately 0.3% water over a 24-hr period, which affects lenses dimensional stability over time. However, there is a class of optical polymers, specially developed for optical applications, COP or COC, with absorption proclivity, lower than <0.01% [53]. These polymers are recommended for high-precision applications since they provide a stable focal length due to their low water absorption and their thermal stability [54]. In contrast, PC is not ideal for high-precision applications due to its relatively high water absorption inducing swelling compromising their tight tolerances [55]. The stress birefringence is also dependent on the type of material, which has intrinsic birefringence associated with its structure. In optical polymers, the stress-optic coefficient is higher than in optical glasses, for this reason, the stress birefringence is more critical in polymers. Each material has characteristic constants of intrinsic birefringence and stress-optic coefficient, as presented in Table 1. For instance, the stress-optic coefficient of COP is lower than the stress-optic coefficient of PC and similar to the PMMA, which in turn will define the different birefringence values and distributions [16].

Beyond the optical properties of materials, replication performance is also crucial. Kalima et al. [56] studied different transparent polymers in the replication of diffractive optical elements using μ IM and, it was established the type of material as the most significant factor. Four polymers were studied, PC, COP, and two other less common, styrene-acrylonitrile copolymer (SAN) and hexafluoropropylene–tetrafluoroethylene–ethylene terpolymer (HFP–TFE–Et). The results showed that replication fidelity was highest with PC and lowest with SAN. Kirchberg et al. [57] studied the replication of microlens arrays during μ IM also with different polymers, PC, PMMA, and PS. The PMMA showed the best results, with good reproducibility of the diamond milled mold insert structure, among the low-cost optical polymers studied, with a surface roughness of 26 nm. The PS showed inferior results, with a larger difference in the surface roughness, i.e. 19 nm, compared to mold insert values of 25 nm. Holthusen et al. [58] compared the filling behavior and replication quality of the most popular optical polymers, PMMA, COP, and COC. The best results were achieved when PMMA was used. The microstructures in COC and COP appeared to be blunt and geometric deviations compared to the mold were higher. Loaldi et al. [59] also support that PMMA had a higher replication degree than COP. This behavior can be explained due to the lower viscosity of PMMA in the range of typical shear rates of IM. This behavior is also depicted in the viscosity plot of Fig. 3. Lou et al. [60] studied the production of microlenses with 150 μm of diameter, 200 μm of pitch, and 13.5 μm of height using PC and PMMA. The moldability of the PMMA was better than PC. The average surface roughness of the molded microlens arrays was 4.50 nm for the PMMA material and 4.61 nm for the PC. Moreover, the residual stress of the PMMA was smaller than PC by birefringence measurement.

5. Injection molding process

IM is the most used process technique for polymer processing. Allows high production rates, complex geometries, dimensional precision, high reproducibility of optics with high accuracy. Typically, the molding cycle is constituted of five steps. In the first step, the mold closes and the injection unit moving forward is followed. Then, the melted polymer is injected, it fills the mold cavity, and after that, in order to compensate the material shrinkage, packing pressure is applied. After packing pressure, the injection unit steps drawback and is initiated the plasticization for the next cycle. The part in the mold is cooled, after reaching sufficient stiffness the mold opens, and the part is ejected [61]. However, IM is the main source of residual stress and warpage in optical lenses, therefore, the production of optical parts with a reproducible quality requires a high degree of process stability and the process parameters must be highly controlled [62].

The residual stresses induced during IM cause different problems in the optical component. The most problematic is anisotropy, which affects optical properties, such as birefringence, and causes loss of mechanical properties. The residual stresses can cause also warpage, non-uniform distribution of refractive index, as well as variations of curvature radius and form deviations. This affects the optical performance since these parameters determine the focal length, location of the main plane, and wavefront aberration. The residual stresses can be divided

Table 1
General physical and optical properties of common optical polymers and glass [16,31,49,50].

Properties	Glass	Polymer					
		PMMA	PC	COP	COC	O-PET	PS
Density (g/ cm^3)	2.51	1.19	1.2	1.01	1.02	1.22	1.05
Water absorption (%)	–	0.3	0.2	<0.01	<0.01	0.15	0.2
Light Transmittance (%)	91	92	88–89	92	91	90	87–92
Refractive index,	1.52	1.49	1.59	1.51–1.53[a]	1.53	1.61	1.59
Abbe number	–	58	30	56	56	27	31
T_g (°C)[a]	+600	100–113	130–150	123–156	134–158	121	100
Birefringence[b]	5	4	2	4	4	4	1
C ($\times 10^{-13}$$cm^2$/ dyn)	2.77	4.5–6[a]	30–72[a]	6.5	4	–	−55
Price	€€€	€	€	€€	€€	€€	€

Abbreviation: T_g, glass transition temperature. *C*, stress-optic coefficient.
– No data is available.
[a] The property value varies within the range of values provided depending on the grade.
[b] Qualitative classification: 1 bad; 5 good.

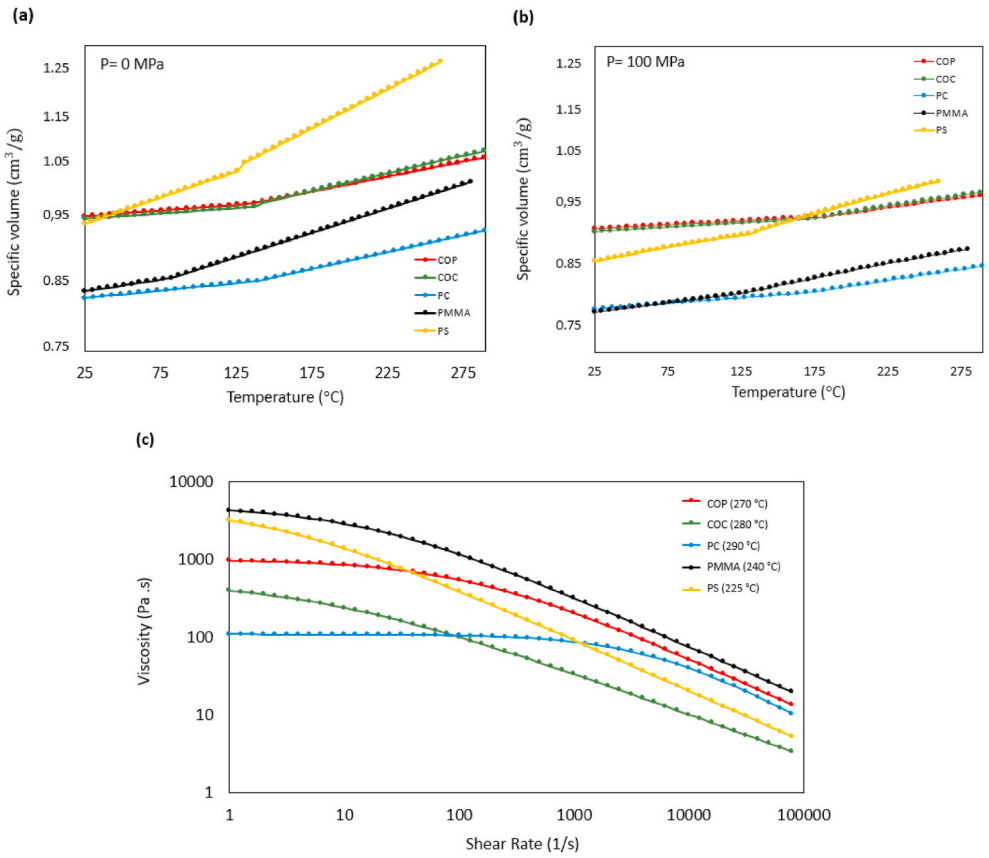

Fig. 3. Optical polymer properties (a) PVT plot (P = 0 MPa); (b) PVT plot (P = 100 MPa) and (c) viscosity dependence on shear rate; of COP (Zeonex®E48R from ZEON©), COC (TOPAS® 5013 from TOPAS Advanced Polymers GmbH), PC (PANLITE®AD5503 from Teijin), PMMA (ACRYPET™ VH from Mitsubishi) and PS (Styron® 693 from Americas Styrenics). Data collected from the Moldflow® software database, version 2021, by Autodesk®.

into two main causes, the flow-induced stresses and the thermally induced stresses, which will be discussed in the following section 5.1 [63,64].

5.1. *Residual stress in injection molded lenses*

The flow-induced residual stress is developed during the filling and packing stage and it is related to molecular orientation, while the thermally-induced stress is developed during post-filling, in the cooling stage [65]. During the filling and packing stage, molecular orientation is a result of the flow direction due to the high shear rate near the mold walls. In the core, the shear rate is lower and the molecular orientation is not so significant. Due to the fast cooling of the melted polymer, in contact with mold walls, the outer surfaces freeze before molecular relaxation occurs, forming a frozen layer, and the molecular orientation is locked. On the other hand, the core is still melted, with a temperature high enough to allow relaxation of the molecular chains. These differences cause residual stress in part. As flow is the main reason for molecular orientation, it is denominated flow-induced residual stress [65]. The mechanism of the formation of flow residual stress is shown in Fig. 4.

The thermally-induced residual stresses occur during the cooling phase due to several reasons. One of them is due to the differences between the frozen layer and the core. There is a constraint on the thermal

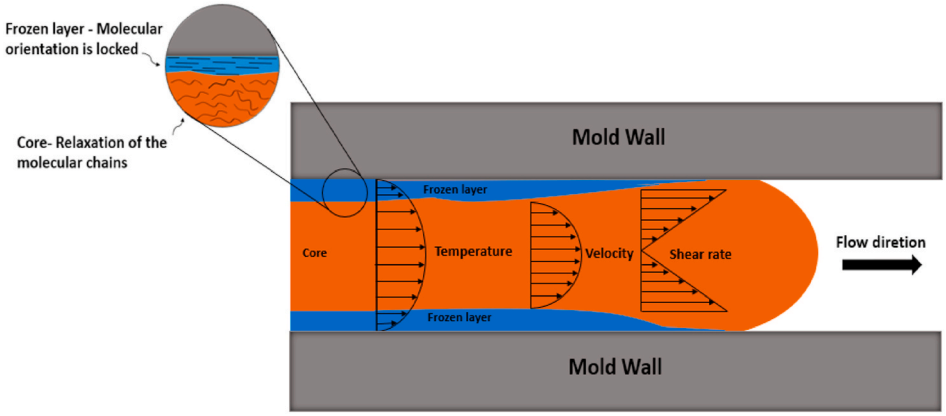

Fig. 4. Flow-induced residual stress during filling.

contraction imposed by the frozen layer. This constraint among layers is one of the sources of thermally-induced residual stress. In the frozen layer there is compressive stress, and the core is under tensile stress. There is an asymmetric tensile and compressive pattern along the thickness, resulting in a bending moment that causes the warpage of the component, generally affecting the mechanical behavior. The thermally induced stress can also be a result of the volumetric shrinkage of the part during IM, which occurs due to PVT change, as the part is cooled from a high temperature to room temperature and high-pressure condition after the packing stage. Different cooling rates across thicknesses in a part, cause non-uniform volumetric shrinkage, which consequently causes warpage and distortion of demolding parts [66,67]. Parts with non-uniform thicknesses, poor cooling systems, or non-uniform cooling systems are more sensitive to thermally-induced residual stresses.

The main effect of warpage in optical lenses is the deviation of the wavefront compromising the lens focus. This phenomenon results in a surface error and, consequently, in wavefront aberration in the lens, as exposed in Fig. 5. An optical axis declination or aberration is induced when refractive indices and the curvatures are different on both sides of the lens. In a lens with undesirable deformation, the rays will converge to different points instead of a common point on the image plane. Consequently, it may result in an optical behavior different from that predicted with optical design [31,68].

The scheme, shown in Fig. 6, summarizes all interactions and effects of IM on mechanical behavior and optical performance of polymer optical lenses. The defects caused by thermal residual stress and flow residual stress are divided by the main source, warpage, and birefringence, respectively. Accordingly, with previous studies, the total birefringence in molded lenses is contributed mainly by flow-induced effects and the thermal-induced residual stress has a lower contribution [15,69].

5.2. Injection compression molding process

ICM is a variant of IM, pointed out as the most accurate technique for high-precision optical components, as it allows enhanced optical performances in terms of birefringence, and replication compared to conventional IM [10]. It combines a uniform pressure distribution and the automation of IM, which results in precision parts with excellent mechanical properties, low residual stress, and tight tolerances. In ICM, the cavity has a large transversal section, which allows the melted polymer to proceed immediately to the end of the cavity under low pressure. During or after injection of the melted polymer into the cavity, the compression step occurs, while the mold is slightly open. The cavity thickness or compression gap is reduced during the mold closing movement, which forces the melt to fill and compact uniformly the entire cavity [10,38]. Fig. 7 shows the steps in the ICM process.

Although, optical lenses may be produced by IM with good quality and accuracy [70], the accuracy obtained by ICM is higher, as reported by Loaldi et al. [59], Wu et al. [11,71], Chen et al. [37], and Michaeli et al. [72,73]. Michaeli et al. [73], compared the maximum difference between mold and lens surface, through peak-to-valley-value (PV-geo). As shown in Fig. 8 (a), ICM, in both surfaces, enables the reduction of PV-geo. Sortino et al. [74] compared the replication of prism patterns typical of Fresnel lenses obtained by IM and ICM techniques. It was concluded that the ICM technique enables the highest replication degrees, reduced results variations, higher structures repeatability, and reproducibility, as shown in Fig. 8 (b). Roeder et al. [75] also support the use of ICM and denote that it is mandatory to achieve high quality. In this study, microlens with microstructures with 4 of height was fully replicated by ICM. The conventional IM process was also conducted but complete parts were not able to be achieved. From ICM numerical simulation, Chen et al. [76] found a decrease in part shrinkage and better shrinkage uniformity. At the same point, the shrinkage index was reduced from 5.2% to 3.1% by ICM. In the same study, it was verified that higher compression speed results in a decrease of shrinkage index and a higher compression gap in larger shrinkage distribution.

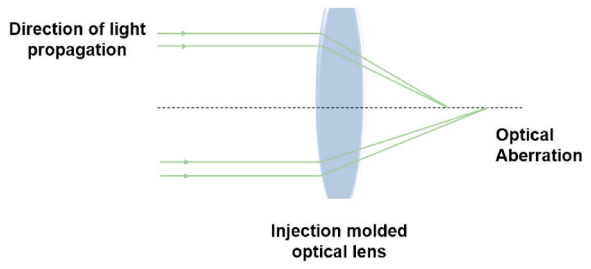

Fig. 5. Schematic illustration of effects of warpage in the induction of undesirable optical aberrations in an injection molded optical lens.

Chen et al. [29] studied the ICM process parameters and concluded that a larger compression gap increases birefringence. Young et al. [77] used numerical simulation to study the effects of the ICM process parameters such as compression force, mold temperature, and compression time on the residual stress of the PMMA lenses. The study demonstrated that, due to the small size of the lens, the compression force does not play an important role. The mold temperature and the compression time were relevant to the uniformity of the residual stress distribution and thickness shrinkage. Furthermore, the residual stress and thickness shrinkage were more uniform by decreasing the compression time, Fig. 8 (c). Chen et al. [78] also reported the effects of the ICM process parameters on the residual stress of plastic lenses and it was established that the compression delay time on the residual stress was the most significant parameter, followed by compression gap and compression speed.

5.3. Effect of process parameters on optical lenses

As mentioned above, process parameters have a high effect on the final quality of lenses. Macías et al. [34] found that an incorrect selection of IM process parameters led to the generation of residual stress in the plastic lens, which significantly affected the structural size of the lens and its dimensional accuracy. The effect of melt temperature is an example, it was shown that it has opposing effects in retardation and warpage. A higher melt temperature results in lower retardation, but superior warpage, and an increased aberration or form error [30]. Consequently, for an effective process, the processing conditions should be controlled. Some studies report the use of the *Design-of-Experiments* (DOE) technique or the one-factor-at-the-time approach to study the effect of a set of process parameters on a response [25,59,79,80]. More recently, commercial software's been used to simulate the IM process and predict the optical properties based on viscoelastic properties and residual stress. In these works, flow rate, injection speed or filling time, melt temperature, mold temperature, packing pressure, and packing time are always the main processing parameters with an impact on residual stress and geometric distortions.

5.3.1. Geometric accuracy and surface quality

In the field of polymer optical lens processing, the studies reported in the literature have focused on the enhancement of geometric accuracy, surface quality, and prediction of defects. In these studies, some authors focused on optimization and improving the size, shape, and accuracy of optical lenses. Pazos et al. [13] estimated the final thickness of the PC biconcave and biconvex lenses using the CAE simulation. Furthermore, superficial defects of the optical lens were analyzed, to estimate the critical thickness versus the number of weld lines and air traps. Hu et al. [81] studied the effect of packing pressure, packing time, and gate size on shrinkage of aspheric lenses. The research shows that packing pressure not only determines the part shrinkage size but also affects the uniformity. When packing time is insufficient to reduce shrinkage it is recommended to increase packing pressure. When the packing pressure was higher than a critical value, the effect on the shrinkage size becomes

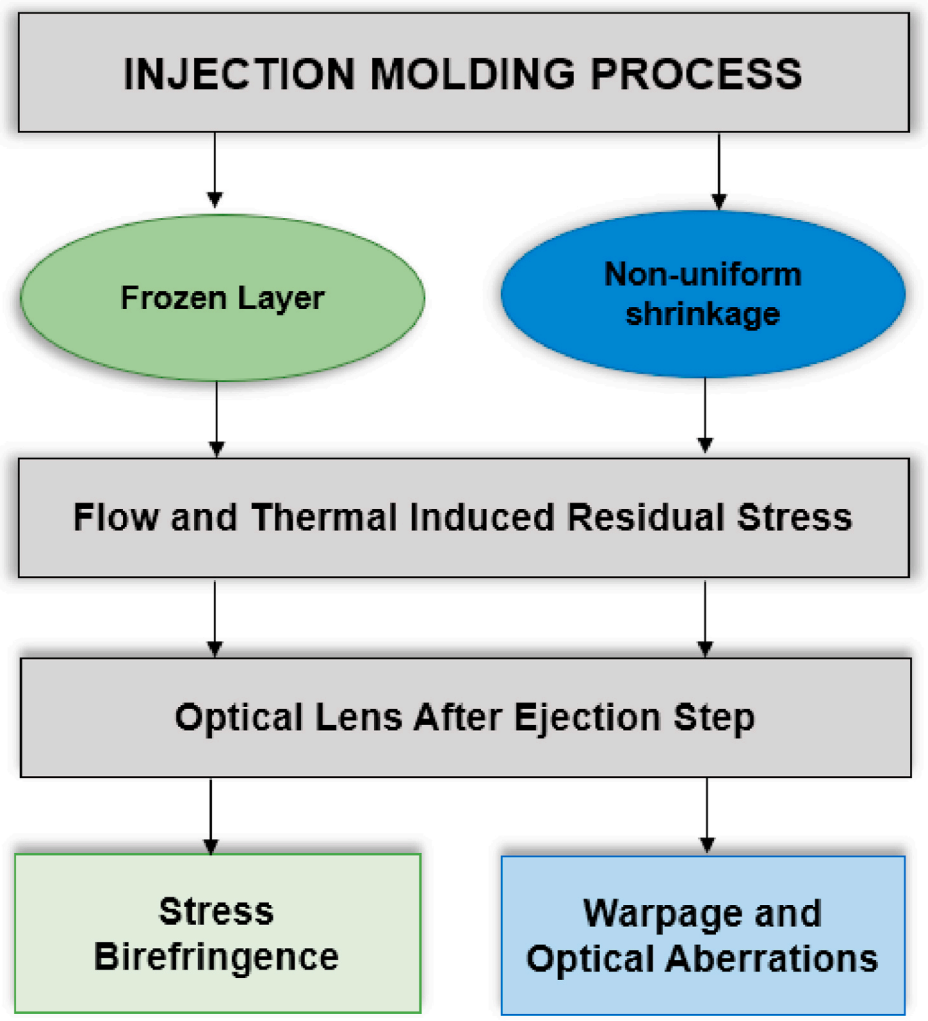

Fig. 6. The effects of IM process in the induction of defects in optical lenses: stress birefringence, warpage, and optical aberration.

smaller and the shrinkage uniformity was guaranteed. According to these authors, the critical value of packing pressure should be found out during the packing profile setting. In practice, packing pressures should be higher, about 5 MPa than the pressure which is added to the theoretic pressure to ensure the packing results.

Lu and Khim [82] through a statistical experimental study investigated the effects of the molding conditions on the surface contours error of molded lenses. It was verified that mold temperature is the most significant process parameter. The results show that the contour error increases 34% with an increasing mold temperature, followed by the injection speed, with an increase of 11%. The effect of packing pressure was not significant for the contour errors, however, it was critical for residual stress with a 50% increase. Furthermore, was proposed the use of two-stage packing pressure to improve the surface replication for the lenses, allowed more material to be packed into the cavities, and provided a better surface replication. Shieh et al. [83], and Bensingh et al. [27] optimized biaspheric lenses and large-diameter aspheric plastic lenses, respectively. Both investigations were conducted through numerical simulation to effectively reduce the volumetric shrinkage. In these studies, the packing stage was identified as the most significant factor for minimal volumetric shrinkage. Through the correct selection of the process parameters, Shieh et al. [83] achieved maximum surface profile errors on the light incident side of 2.12 μm and 2.37 μm, which is below the commercial manufacturing specification of the lenses under study (2–5 μm). Bensingh et al. [24] identified the packing time as the most important parameter. The surface roughness achieved on the lens was 53.2 nm compared to the surface roughness of the mold inserts of 51.6 nm. Yin et al. [84] studied thickness distributions under various process conditions in lenses produced by μIM. The lens overall thickness decreased gradually in the main flow direction, while almost kept unchanged in the cross-flow direction. The local thickness of the lens tended to decrease in the melt filling direction. Moreover, the research also identified the packing time as the most important parameter to achieve a uniform thickness. The uniform thickness of the molded lenses was evidenced by a small thickness standard deviation value of 12.24 μm.

In the convex or concavity of aspheric lenses, the volumetric shrinkage was found higher in the center of the lenses, which is the most significant region. The warpage was higher in this area. In the remaining areas, the volumetric shrinkage decreases gradually and the minimum volumetric shrinkage appears at the injection location [26,85]. Tsai et al. [24] studied the influence of the IM process parameters on the optical quality of small-diameter plastic lenses. In this study, it was established the process parameters have only a slight effect on surface roughness. Between all conditions, a small difference of 4–5 nm was observed. The final surface roughness of the lens is primarily the result of the mold surface quality. The surface waviness was also investigated and the melt temperature and packing pressure were the most significant parameters. The surface waviness may be improved with higher melt temperatures, injection pressure, packing pressure, and mold temperature. Zhang et al. [86] studied the accuracy of thin-walled COC microlens arrays using μIM. The geometric accuracy (height, sphere

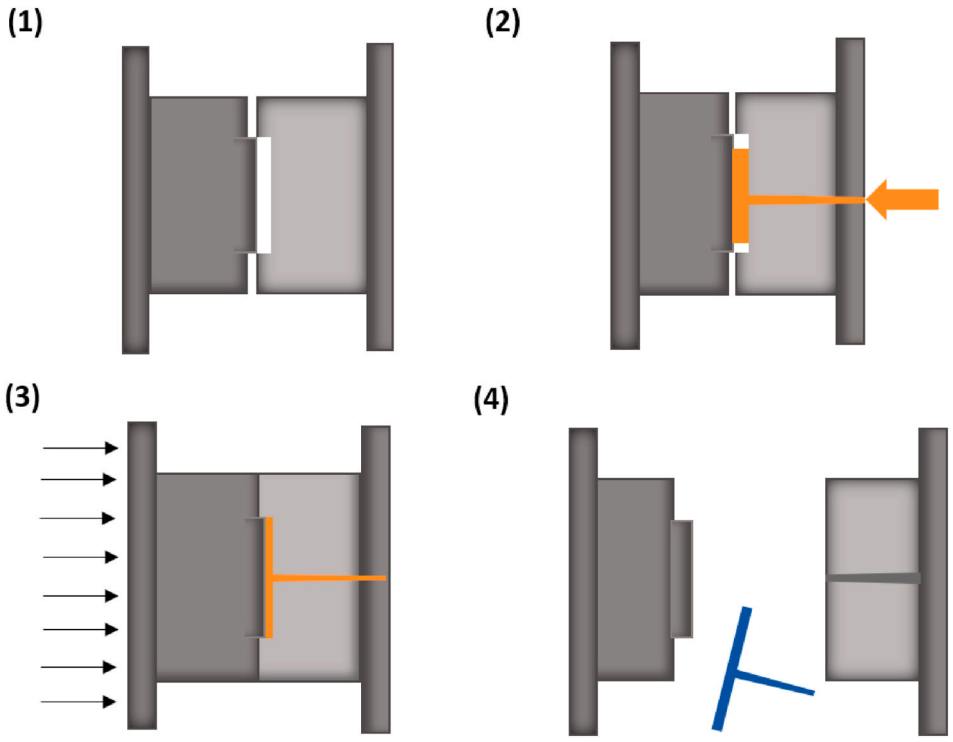

Fig. 7. ICM process scheme: (a) Closing the mold; (b) Filling step; (c) Compression step (d) Cooling and ejection step.

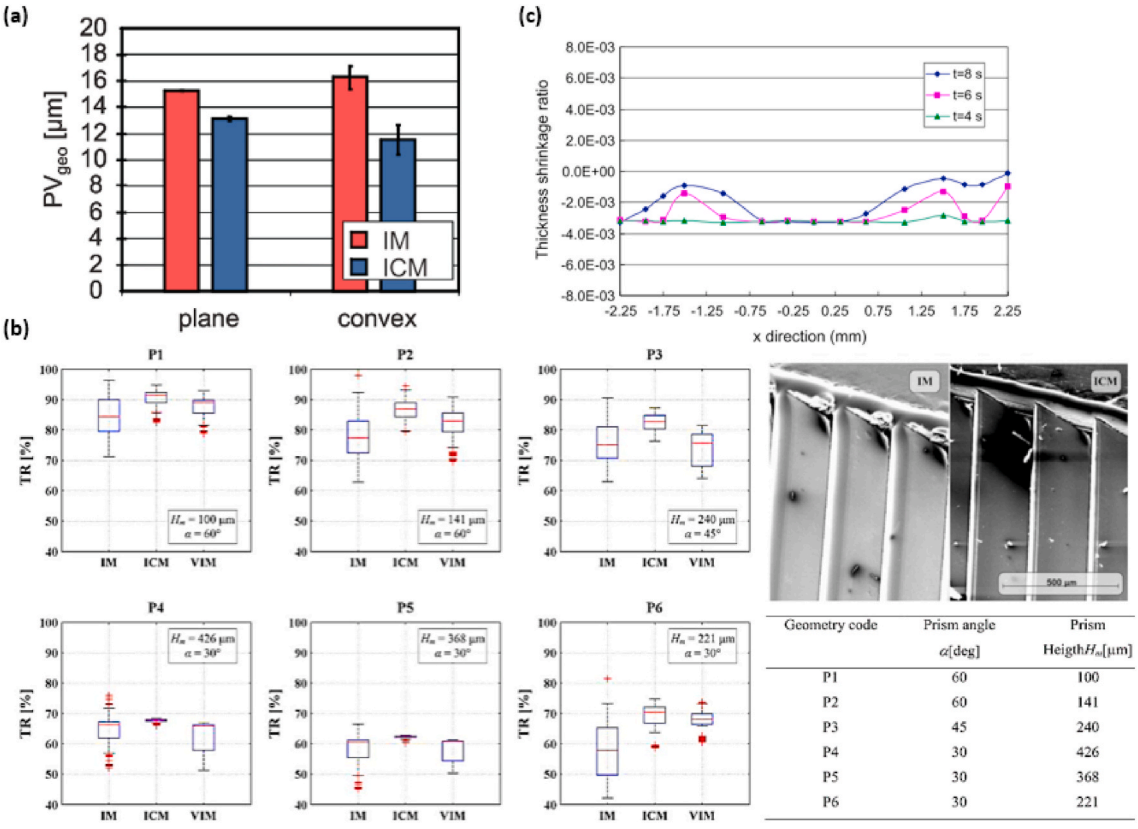

Geometry code	Prism angle α[deg]	Prism Height H_m[µm]
P1	60	100
P2	60	141
P3	45	240
P4	30	426
P5	30	368
P6	30	221

Fig. 8. Injection compression molding: (a) geometric accuracy between mold and lens surface of the optical lenses compared to the IM. Reprinted with permission of [73]; (b) Transcription ratio (TR) of prisms compared to the IM. Reprinted with permission of [74]; (b) (c) uniformity of thickness shrinkage by reduction of compression time. Reprinted with permission of [77]. Copyright © 2021, Elsevier.

radius, form error, pitch between adjacent microlenses) and surface quality (surface roughness, waviness, and PV) were analyzed through a DOE. For the height and form error, the interaction of packing pressure and the mold temperature was the more important. Regarding surface quality, the mold temperature demonstrated a major effect on surface roughness and PV, while the interaction of injection speed and melt temperature was more important for waviness. Overall, the surface quality was mainly influenced by differences in cavity temperature, which was a combined effect of mold temperature and melt temperature.

In the field of optimization of the process conditions, a recent approach has been proposed, emerging as a new trend with the potential to achieve the optimal quality of optical lenses. Applying artificial neural networks (ANNs) to predict the optimal process parameters, combined with other methods, e.g. genetic algorithm or particle swarm optimization, enables to rapidly obtain the optimal process parameters according to the required quality of the optical lenses. These recent methods have been used to minimize the volumetric shrinkage variation in aspheric lenses [87], optimize the accuracy and geometric deviations [88].

5.3.2. Refractive index

In optical lenses, another important property is the distribution of the refractive index across the lens. This property is intrinsic to the material but also may be affected by molding conditions. It needs to be uniform over the thickness and on the surface. However, in the IM, the melted polymer is cooled from the superficial layer, i.e. frozen layer, to the core, temperature and pressure distributions occur, resulting in irregular shrinkage, and consequently in density and refractive index distribution. Yang et al. [89] and Li et al. [90] studied the influence of packing pressure in the refractive index of injected PMMA lenses. The process simulation demonstrated that increasing packing pressure reduces or eliminates density variations. When a higher packing pressure was used, a more uniform distribution of the refractive index was achieved. Low packing pressure caused more density variations on the lens.

5.3.3. Birefringence

Chang et al. [15] studied the prediction of birefringence by numerical simulation of aspheric lenses and concluded that birefringence is mainly due to flow-induced stress. Flow-induced fringed order and the thermally-induced fringed order were compared and it is shown that the flow-induced fringe order is significantly larger than the thermal-induced fringe order. Furthermore, maximum shear stress at the end of the filling, obtained by the numerical simulation, was correlated to flow-induced birefringence pattern and showed that the distribution is similar. It was verified that the maximum shear stress is largest near the gate and decreases with distance from the gate. The same was verified to the birefringence, measured experimentally with a distribution similar to predicted by numerical simulations. Further studies are in agreement that birefringence maximum arising near the gate of part [91].

Weng et al. [35] studied, experimentally and through simulation, the influence of the melt temperature, the mold temperature, the flow rate, and the packing pressure on residual stress and showed the mold temperature is the most significant processing parameter. The maximum residual stress was lower when the mold temperature was higher. A higher mold temperature reduces the cooling rate of the frozen layer, resulting in more uniform cooling throughout the entire thickness. The effect of mold temperature on residual stress is well supported and has been reported by other researchers [77,92]. Furthermore, the same authors establish in this work, and in a previous work [36], that prediction of residual stress numerical simulation by finite element only works properly from a qualitative point of view, as shown in Fig. 9 (a) and (b), respectively. The authors explain the differences between experimental and simulated values may be due to stress relaxation during the cooling stage, viscoelastic stress relaxation, simplifications of the numerical simulation models, and the ambient environment during the measurement. Even so, numerical simulation is still an effective and low-cost approach to optimize the optical performance of polymer molded lenses.

Lin and Hsieh [28] optimized the birefringence of PMMA Fresnel lenses through numerical simulation. It was shown by properly setting the processing parameters, the average residual stress may be reduced by 75.1%, which results in a reduction from 6.848×10^{-5} to 1.731×10^{-5} in the average birefringence, and represent a reduction of 74.7%. Employing a Taguchi robust design method, the processing parameters studied were ranked in order of descending influence: melt temperature, filling time, packing time, and mold temperature. It was defined that the melt temperature has a positive effect on birefringence, while packing time has a negative. Lin and Chen [68] studied the influence of processing parameters on residual stress and warpage of PMMA double-convex Fresnel lenses. The study demonstrated that the processing parameters which simultaneously minimize the warpage and the residual stress, may be ranked as follows: melt temperature, lens thickness, packing pressure, cooling time, mold temperature, and gate location. Given the optimal process parameter settings, the warpage and retardation are reduced by 60.82% and 66.82%, respectively, compared to the original conditions, as shown in Fig. 10.

On the other hand, the same authors in another study found that the packing stage has more influence when simultaneously is optimized the warpage and the retardation of the asymmetric plastic double-convex Fresnel lenses. The Taguchi experiments were used to determine the most influential processing parameters, followed by a grey relational analysis technique, applied to the Taguchi results to establish the pro-

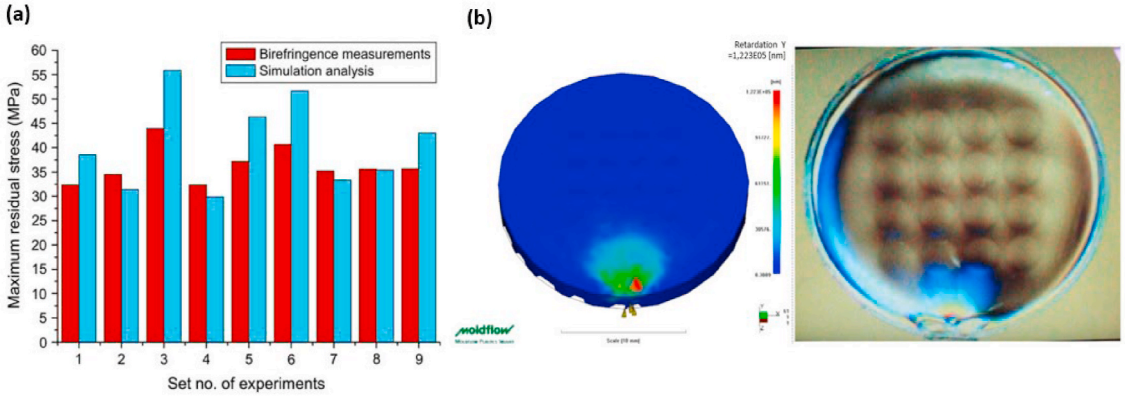

Fig. 9. Comparison between simulated and experimental of (a) maximum residual stress of the PC microlens array. Reprinted with permission from Ref. [32]; (b) Good agreement, in qualitative point of view, of residual stress distributions by simulation and experiments of the PC microlens array. Reprinted with permission from Ref. [36]. Copyright © 2021, Elsevier.

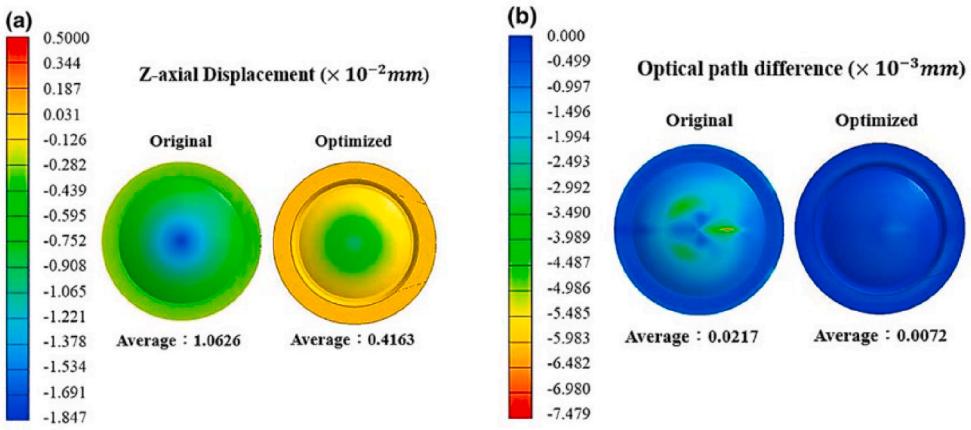

Fig. 10. Optimization achieved by Lin and Chen, through numerical simulation: lens warpage distribution (left) and retardation, or optical path difference (right). Reprinted with permission from Ref. [68]. Copyright © 2021, Springer Nature.

cessing parameters that achieve the ideal trade-off between the two performance goals. The results showed that the control factors may be classified in descending order of influence as follows: packing pressure, packing time, melt temperature, filling time, cooling time, and mold temperature. Through this optimization, the warpage was reduced from 54.6 μm to 46.9 μm which represents an improvement of 16.42%, while the retardation was reduced from −106.1 to −26.8 μm, which represent an improvement of 74.74% [30]. Lin and Chen [27] explain that the differences between this study and the previous one may be due to differences in the symmetry designs of the two lenses.

5.4. Effect of the gate and runner design on optical lenses

As mentioned before, the shear stress at the end of filling has a huge effect on birefringence, hence, the gate design and gate size must be considered. In optical applications, it is recommended to use a lateral gate to avoid marks on the optical surface. Many authors have studied numerically and experimentally the effect of gate size in shear stress and birefringence and found that large gates significantly decrease birefringence [4]. To avoid shrink marks and voids, especially during the production of lenses, the shrinkage of the material needs to be balanced by the injection of additional material during the cooling period. The diameter of the runner needs to be a sufficient size to prevent the sprue from freezing too early. Lin et al. [93] analyzed and optimized the geometric parameters of the optical lens gate and found that large gate thickness, length, and inlet width allowed the reduction of the average residual stress. Furthermore, it was determined the influence of geometric parameters of the gate in order of diminishing influence followed by gate thickness, gate length, gate inlet width, and gate outlet width.

In general, it is established in the literature that runner design affects the polymer molecular orientation, the melt front stability, and hence affects the lenses quality. Thus, to ensure the quality of circular optical lenses, it was proposed by Bu et al. [94] a runner structure with two gates. The first gate with a shorter length and lesser sectional area connects the runner. The second gate had a longer length and lower height, its sectional area was relatively larger than the first gate, and in the middle of this gate, there was a narrow *bayonet-type*. When the melt passes the first gate due to the sudden decrease of sectional area, the melt velocity becomes fast, thus causing great shearing stress, increasing the melt temperature, and further homogenizing. After that, the melt goes through the second gate, which is larger, slowing down the material, becoming a laminar shape, and entering into the cavity. Through this structure, the molecular orientation of melt in the cavity decrease, improving the quality of the lens. Tsai [23] studied the runner design to improve the optical lens quality and concluded that the melt temperature is evenly distributed when a restrictor is installed on the tertiary runner. The developed method enhanced the contour accuracy from 10.44 to 5.025 μm, which represents an improvement of 51.9%. The comparison of experimental and simulated results was also conducted and an error of 49.6 and 66% for runners without and with a restrictor parallel to the injection direction, respectively, was achieved. According to the authors, the relatively large errors were derived from the coarse mesh size of the simulation and the inherent error of the simulator. In another study, Tsai and Lin [95] also found that warpage is affected by gate design and runner since it enables melt front stability and hence a uniformity temperature and pressure distribution. The result obtained suggests that the optimized runner design is a cylindrical-shaped restrictor in the secondary and quaternary runners, with the restrictor end aligned with the tertiary runner edge and fan-converge shape gate. The surface contour was reduced to 57.91 μm and improved by 28.6%. A comparison of simulations and experiments was also conducted. The simulation prediction is consistently higher than the experimental values, however, with a small error of 10.5%, which reveals a good simulation prediction when properly prepared.

6. Functional coatings

6.1. AR coatings

Currently, a plethora of optical technologies is strongly based upon the knowledge of light-matter interactions. By combining materials with different refractive indices, establishing a suitable geometry, and/or fabricating nanostructures on the surface of a substrate, it is possible to control the light pathway in a solid system, to select the wavelengths able to propagate through a given medium [96] and also, to explore the interactions between the radiation and light-emitters confined within resonant solid-state optical cavities [97–99]. With regard to lenses with optical coatings, great progress has been observed in the last decades, which can be considered a historical mark in the field of optics. In particular, AR coatings have had a great impact on technical optics. In some applications, AR coatings are simply required for the reduction of surface reflection, whereas in others, they are used to also increase transmittance. For instance, lenses with AR coatings are employed in cameras or LiDAR systems. Due to the sensitivity of such systems, they demand higher levels of light to respond adequately. Hence, AR properties are required to increase transmitted light to improve the contrast of displays and avoid the formation of ghost or veiling glare images.

AR coatings in glass substrates have been well established for many years, while the interest for AR coatings in polymers has grown in the last decades. However, AR coatings on polymeric substrates still present some challenges. In contrast to glass, the use of polymeric substrates limits the temperature of the deposition processes. Mechanical and

thermal properties of polymer substrates differ from those of inorganic thin-film materials. In addition, different polymeric substrates present different chemical and surface compositions, which can lead to various chemical reactions when in contact with other chemicals or plasma-assisted deposition processes. As a consequence, AR coatings usually suffer from poor wear resistance and poor photostability, with the adhesion of the deposited thin film on the polymer substrates being affected. To enhance the adhesion, several methods have been explored to modify the polymer surface, such as plasma treatment using different gases [100,101], irradiation with an ion beam [102] or excimer laser, and spin-casting organic solvents. For more details about the properties and coating adhesion of the most commonly used rigid thermoplastics for optical components, the reader is referred to the work of Piegari and Flory [103].

6.1.1. Basic concept for reducing reflection

The reduction of reflection can be achieved by exploring, in a controlled manner, the interference phenomenon in thin films. The basic concept lies in the correct choice of the refractive index and thickness of the films. To clarify, a simple case is considered, as depicted in Fig. 11 (a), formed by air, a thin film, and a substrate, where n_0, n_1, and n_2 are the refractive indices of air, the film, and the substrate, respectively, and the thickness of the thin film is d. The relation between the refractive indices is. $n_0 < n_1 < n_2$.

It can be seen that after reaching the system, the incident light is divided into two rays: one is reflected in the interface air/thin film and the second is reflected in the interface of the thin film/substrate. The difference in the length followed by each of the reflected rays is:

$$\Delta L = 2d\cos(\theta) \tag{8}$$

where θ is the angle for the incident light. The ΔL gives rise to a phase difference between the reflected rays, φ. It is also important to consider that ΔL takes place in a medium with a refractive index n_1, where the light speed is slower than in the medium n_0. When the two reflected wave-fronts are completely out of phase, destructive interference takes place, canceling out both the rays entirely and thus enhancing the transmittance. To obtain an AR response from the system, the conditions must be: i) the two reflected waves must be exactly 180° out of phase and should be of the same intensity after reflecting at two: ii) the film depth should be an odd number multiple of one-fourth of the incident beam ($\lambda/4$). The equation governing the reflection of the system at normal incidence is:

$$R = \left(\frac{n_0 n_2 - n_1^2}{n_0 n_2 + n_1^2}\right)^2 \tag{9}$$

Since it is intended that $R = 0$, Eq. (9) returns in:

$$n_1 = \sqrt{n_0 n_2} \tag{10}$$

which establishes the condition to achieve index matching. A more detailed discussion is done by Raut et al. [104].

In Fig. 8 (b) we have a multi-layered system or AR coating, which is a more complex system once the incoming light goes through an increased number of layers with different refractive indices. Higher levels of AR responses are observed in systems like this. Normally, the multiple layers are arranged interleaving materials with high (n_H) and low (n_L) refractive indices and adjusting the thickness of each one, it is possible to achieve a similar behavior as described by Eq. (12), in which the light is guided throughout the whole system. The efficiency of such systems will strongly depend on the number of layers and contrast of the refractive indices that can either be deposited on one or both surfaces of the polymers.

6.2. Other functional coatings

Many technologies based on the use of polymers may be improved by combining these materials with coatings and/or surface modifications. Nevertheless, the use of polymers still present limitations regarding adhesion and wettability. These issues are typically originated from different factors such as, impurities that arise during the polymerization process, the presence of polymer tails with low molecular weight, the use of additives (e.g. antioxidants or mold release agents), as well as post-processing contaminations [105].

Different surface treatments have been used to increase adhesion, such as plasma (e.g. O_2, N_2, and Ar), sputter etching, and UV/Ozone. Kitanova et al. [106] compared the effects of RF plasma treatments of Ar, and Ar/C_2H_5OH to those of O_2 and gas mixture with different ratios of Ar/O_2 on the free surface energy, morphology, and optical properties of polycarbonates. The adhesion of plasma deposited SiO_2 thin films after the treatments were evaluated through cross-cut and pull-off tests. The authors observed higher adhesion due to the increase of the hydrogen bonding in the substrates that were treated with a 3:1 Ar/O_2 gas mixture for 5 min. Substrates treated with O_2 plasma showed higher roughness and poor adhesion. Fujimani et al. [107] studied the effect of sputtering cleaning on the chemical bonding in the interface

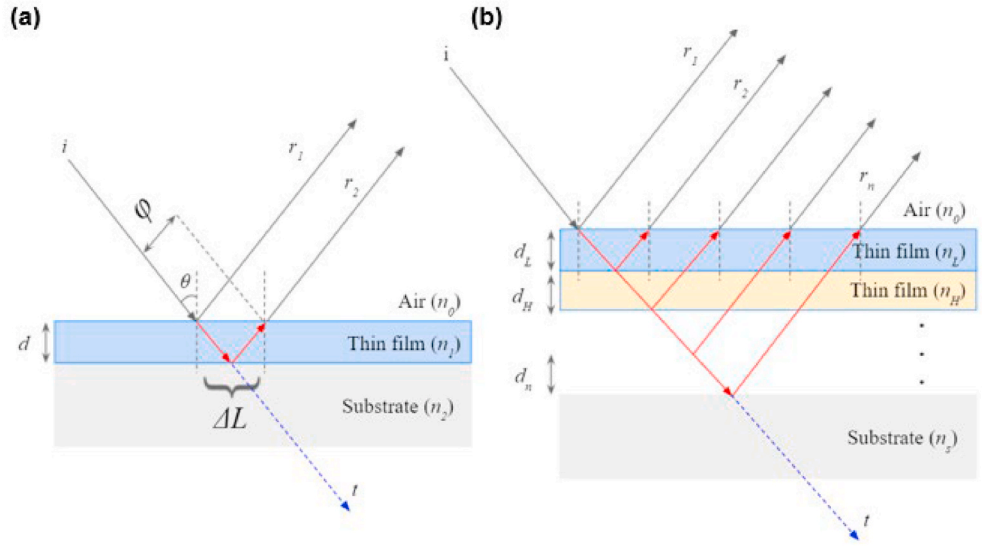

Fig. 11. Schematics representing AR coating: (a) based on a single layer and (b) multilayer coating.

metal/polymer. Thin films of Ti were deposited on polyethylene and polytetrafluoroethylene substrates either treated or non-treated for reasons of comparison. The sputtering cleaning treatment was conducted using Ar ion irradiation at 0.3 keV. Regardless of the substrate, the adhesion was higher in those treated with sputter cleaning as was revealed in measurements of pull strength as functions of carbon-metal bonding ratio and fluorine-metal bonding ratio. UV/Ozone is another extensively used treatment to increase polymer adhesion. This technique allows the generation of high-energy photons that can be used to break C–C bonds and cause chain scission and crosslinking mechanisms in the surface of polymers, as reported by Peeling & Clark, 1983 [108]. Hamdi et al. [109] reported their results on the adhesion modifications of commercial polymers, named ethylene propylene diene methylene (EPDM), polyvinyl, and acrylonitrile butadiene styrene (ABS) chloride (PVC) after UV/Ozone treatment. All the samples were exposed to UV light in combination with ozone gas, during different times, at room temperature, and at a fixed distance of 35 mm from the UV source. T-peel measurements were performed before and after the treatments. Before, the adhesive properties of all materials were low, after the 3 and 10 min of treating EPDM showed no alteration, however, PVC and ABS adhesion significantly increased.

The deposition of coatings and/or surface treatments can be used to modify the wettability properties of their surfaces [110], thus promoting the enhancement of adhesion between the polymer and other materials [111], as well as increasing the resistance to abrasion [112]. One of the most studied properties of surfaces is wettability; it describes the way surfaces interact with liquids, most commonly water. It is noteworthy that wettability plays an important role in polymeric systems, once a great effort has been done in order to create solutions that confer self-cleaning properties to the polymer surface. The property of self-cleaning can be achieved by two different routes, i.e., either making the surfaces super-hydrophobic or hydrophilic. The cleaning response is then achieved based on the way that the water droplets interact with the contaminants (dirt, particles, adsorbed material, etc.) present on the surface. Mattaparthi et al. [113] observed superhydrophobic behavior by replicating the patterns of leaves on polymeric samples. They applied a two-step soft-lithography process to transfer the patterns of leaves to the surface of a PDMS polymer. By doing that, the authors were able to mimic the hydrophobic behavior of actual natural leaves. Water contact angle measurements returned values as higher as 140°. Xu et al. [114] observed non-wettability response by spin-coating nanoparticles of fluorosilane modified silica (F–SiO_2) on polymeric substrates. The authors reported contact angles greater than 150°. Scanning electron microscopy and atomic force microscopy images revealed that the particles were closed packed thus minimizing the substrate exposed to the environment. The optical properties of the samples were not affected by the nanoparticles film and their transmittance was around 95%. Latthe et al. [115] have studied the effects of SiO_2–TiO_2 coatings on polymers and observed the formation of a very thin layer of water on the resulting hydrophilic surface of polycarbonate samples, which could easily wash off dirt particles. Different volume rates were tested, whereas 7 vol% of SiO_2 in TiO_2 showed smooth cracked free surface morphology and, contact angles less than 10° after 30 min of UV irradiation. Furthermore, the coating showed good transparency in the visible range of wavelengths.

Similarly, Fateh et al. [116] also demonstrated that the mixed metal oxide (TiO_2/SiO_2) can enhance the photocatalytic performance of surfaces by improving adsorption and increasing the amount of hydroxyl groups formed on the surface. They studied the resulting wettability, adhesion, and mechanical stability by means of FTIR spectroscopy, ellipsometry, adsorption (Bruner-Emmett-Teller (BET)), AFM, XRD, and water contact angle. They concluded that the addition of SiO_2 improved the photocatalytic activity of TiO_2 films.

6.3. Deposition techniques

Among the available deposition techniques, physical vapor deposition, and in particular evaporation and sputtering are the most used techniques for manufacturing optical coatings. In this review, we briefly discuss the deposition techniques based on vacuum technologies and sol-gel coating. For a more complete description, the reader is referred to the reviews by Mavukkandy et al. [117], Schulz et al. [118], and Raut et al. [104]. Table 2 summarizes the deposition techniques discussed here.

Evaporation of oxide materials is considered the most commonly used method for producing optical coatings [118]. However, the relatively high temperatures needed to vaporize the target material, make its application to polymeric substrates limited. On the other hand, sputtering deposition is a non-thermal physical vapor deposition method widely used to deposit thin films on substrates. It is based upon ion bombardment of source material, the target. The most common approach for growing thin films using this technique is the use of a magnetron source, in which positive ions present in the plasma of a magnetically enhanced glow discharge, bombard the target. This process has been used for optical coating deposition because it benefits from their intrinsic high stability and homogeneity of the refractive index in the depth of the layers [103]. Due to the high stability of sputtering technology, deposition of a few nanometers is possible with good accuracy for metal-dielectric absorbers.

Chemical Vapor Deposition (CVD) involves the reaction and deposition of volatile precursor(s) on a heated substrate in vacuum. The reaction product, which is a solid, deposits on the surface forming the film. Plasma-Enhanced Chemical vapor deposition (PECVD) used microwaves (MW) or radiofrequency (RF) plasma for activating the reacting gases [118]. The use of organic materials for deposition leads to some factors to be considered. First, organic materials often have lower evaporation temperatures than many inorganics, and consequently, the process requires less effort than required for metals or oxides. On the other hand, the organic molecules in the gas phase are also often more complex and can act as a precursor in the CVD process [103]. Plasma impulse chemical vapor deposition (PICVD), in which plasma excitation is gained by coupling microwave power in a pulsed process, is being used for producing coating light reflectors and eyeglasses [119]. For optical multilayers, PECVD is reported as a process that does not deliver thickness accuracy and homogeneity as good as PVD processes [118]. However, multifunctional coatings, combining AR, anti-scratch, and easy-to-clean coatings were developed on PMMA and PC substrates using PICVD [119].

The deposition of AR coatings using wet-chemical processes typically comprises single-layer or two-layer systems and the preparation of

Table 2
Summary of different deposition techniques used to create AR coatings.

Deposition Technology		Observations
Physical Vapor Deposition (PVD)	Evaporation Sputtering	- Uses relatively high temperatures; - Non-thermal method; - Suitable to polymeric substrates; - Almost unlimited materials selection for the substrate and coating;
Chemical Vapor Deposition (CVD)		- Materials used as precursors are limited and need careful handling; - Suitable for multi-layer coatings; - Suitable for polymeric substrates at controlled temperatures; - Challenging to produce multi-component materials;
Sol-gel coating		- Multilayer preparation is complex and time-consuming; - Complex geometries are not suitable. - Processes can be performed at low temperatures (e.g. room temperature); - Appropriate for large areas formation;

multi-layers is complex because the deposition and hardening steps need to be repeated many times. Nevertheless, sol-gel coating process has been industrially used to produce AR porous coatings [104]. For instance, porous PMMA film [120], two-layer AR coating containing polymerizable nanoparticles modified with alkoxy-silanes and a photo-initiator [121], or a multilayer composed of TiO_2 and SiO_2 for photo-voltaic applications are a few examples that use sol-gel technique [122, 123].

To coat a sol-gel, dip-coating and spin-coating are frequently used. In dip-coating, the substrate is dipped and withdrawn from the desired solution at a controlled rate. The spin coating is a simple process for rapidly depositing thin coatings onto relatively flat substrates. A typical process involves depositing a small puddle of the film material onto the center of a substrate and then spinning the substrate. Centrifugal force causes the film material to spread, and eventually reach the edge of the substrate leaving a thin film on the surface.

6.4. Characterization of the coatings

Characterization methods are of great importance, not only to control optical and mechanical properties and tribological performances but also to test the environmental resistance of coatings to assess their durability. In the last decade, enormous progress in advanced characterization techniques and methods available for coating characterization and testing has been achieved. Various reviews reported in the literature focus on the different techniques used to characterize coatings, such as polymer coatings [124,125] and wear-resistant hard coatings [126]. Here, is given a brief overview of the techniques mostly employed for characterizing AR coatings.

For the characterization of AR coatings, it is of utmost importance to access information about optical and morphological features. Refractive index, reflectance, transmittance, absorption, and surface roughness are the essential parameters normally investigated. For that purpose, spectrophotometry is generally applied for characterizing reflectance, transmittance, and absorption behavior within a specific range of wavelength, depending on the field of application, as can be seen in Refs. [127–129]. Optical or contact profilometry and interferometry are techniques used to study the roughness and thickness of thin films [130]. In addition, ellipsometry is also applied to obtain the refractive index, coefficient of extinction (k), and film thickness using widely known optical models, such as Cauchy, B-spline, or Sellmeier. More information concerning the process of modeling ellipsometric variables can be found in Refs. [131,132] their variables can also influence the optical response such as the adhesion between the AR coating and the polymeric substrate, as it is related to both film-substrate interfacial interactions and internal stresses within the film [124]. The knowledge of the aforementioned variables allows to control the optical quality of each layer present in the coating structure and their interactions with the substrate.

Besides the mentioned methods for characterizing optical properties, other methods can be employed to characterize the chemical composition and microstructure, mechanical and tribological properties, as well as thermophysical properties. For instance, nanoindentation has become a standard technique for the determination of the hardness and elastic properties of hard coatings [126]. For geometrical characterization, the prevailing approaches are typically based on microscopy, namely scanning probe microscopy (SPM) with its variants of atomic force microscopy (AFM) and scanning tunneling microscopy (STM). Cross-sectional geometrical analysis of multilayer stacks is also convenient for different purposes. A focused ion beam (FIB) cross-section was employed to investigate thermal cracks existing due to significant differences between the coefficient of thermal expansion (CTE) of the coating and substrate material.

Chemical composition and structures are typically measured using X-ray photoelectron spectroscopy (XPS), Raman spectrometry and Fourier transform infrared spectroscopy (FTIR), whereas crystallinity and orientation of the films are measured by high-resolution X-ray diffractometer (XRD).

7. Replication of microstructures in optical lenses

Optical components, such as microlens arrays, structured lenses, e.g. Fresnel lenses, or lenses with AR structures, require a successful and accurate replication of features during the manufacturing process and acceptable peak-to-valley. Optical components containing features with several dimensional scales, from μ m to 500 μ m [133–136]. In the last years, this has been a great challenge and has received much attention. The literature on this topic reflects the many attempts seeking to overcome the process limitation [137]. The most studied replication techniques are hot embossing [138–142] and IM, and variants. IM is the most promising technique, in terms of cost-benefits in the production of high-precision lenses, when compared to hot embossing. Usually, it is used μ IM [143], which is a variant of IM. The process steps of IM are shown in Fig. 12. This variant is indicated for the production of low-weight parts (of the order of a few milligrams), which is the case of the most optical lens, and parts that require microscale precision, as micro thin-wall parts [144,145].

The process is similar to conventional IM, however, with some modifications. Often, mold inserts or stamps are required to produce microstructured features, and the injection machine has a few differences. Normally, are used electrical or electro-pneumatic machines with clamping force lower than 15 tons [146]. Either the process starts in the same way, firstly, the melt polymer is injected inside the mold cavity by high injection speed and pressure and acquires the contour of the microstructures of the mold insert. After that, the part is cooled, although the cooling rate is extremely high because of the thin features employed. Finally, the cooled part is ejected [147].

Another, and widely used process to improve replication that derivates from IM, is ICM as explained in Fig. 6. It combines two concepts and their advantages: IM and compression molding; the same principle of hot embossing, and providing automated production of high accuracy parts with low residual stress. The best technique to produce high accuracy microlenses with microstructures combines μ IM and ICM and it is known as microinjection compression molding (μ ICM) [148,149]. In this technique, the process starts with the injection of the polymer into the cavity, about 80–95% of the total cavity volume, while the mold is not completely closed, with a compression gap. After the injection phase, the compression stage occurs. The addition of the compression stage allows overcoming the hesitation effect of the material at the entrance of the micro features. In terms of cost, ICM or μ ICM process requires a more complex mold design, peripheral equipment, and process control, when compared to IM or μ IM [148].

7.1. Effect of process parameters in replication

The most influential stage during on replication of microstructures is the filling since the replication is strongly related to the polymer viscosity. Consequently influenced by temperature and shear rate [150–155]. The melt temperature significantly influences the viscosity and subsequent flow and filling behavior of the polymer melts. Higher melt temperature lowers down the viscosity in filling and significantly improves the replication. However, it is important not raising the temperature too much, since high temperatures thermally degrade the polymer structure, whereby their mechanical and optical properties are dramatically reduced. Similarly, high injection speeds lead to high shear rates, and hence viscous heating, and a higher heat transfer convection, as result, the melt temperature increases and the viscosity decreases. Besides, high injection speeds increase the cavity pressure, which drives the flow into the microstructures. Nevertheless, mold temperature is still the most important parameter in controlling the replication of microstructures as it can reduce the frozen layer and improve the filling [156–158]. It is reported in the literature that a 50% increase in mold temperature may lead to an increase of about 300% in the average

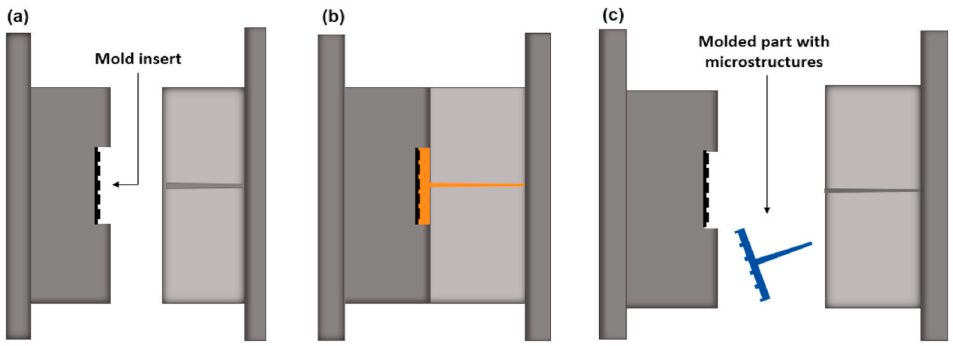

Fig. 12. Schematic illustration of μ IM (a) microstructured mold insert inside the mold cavity (b) injection and packing step and (c) cooling step followed by ejection of molded part with microstructures.

height of microstructures [159]. The packing pressure and packing time also have been studied as well and have also been shown to have a positive effect, however, these parameters are dependent on temperature and the formation of the frozen layer during the filling stage. If the mold temperature is below the *Tg*, increasing the packing pressure has nearly no effect on the replication degree [154]. In a study by Luchetta et al. [160], varying mold temperature from 60 to 100 °C resulted in the average height increased from 0.37 to 1.14 μm, which represents an improvement of approximately 62%. The effect injection speed and packing pressure is far less important. An increase in packing pressure increase by 50% the average height. The variation of injection speed was the less significant, a rise in injection speed only improved the height of the structures by 16%.

Chen et al. [161] investigated process parameters on the uniformity of the height of the microlenses in a microlens array. The melt temperature, mold temperature, injection speed, and packing pressure, were found to have a significant effect. The melt temperature had the most significant effect, while the cooling time had the smallest. Furthermore, in this study, the influence of packing pressure, and injection speed were investigated over a larger range, as represented in Fig. 13. It was shown that the increase of packing pressure enables the enhancement of the uniformity of the height, once it prevents the melt from flowing back and compensates for the reduction of volume due to the shrinkage. However, excessive packing pressure may cause an uneven distribution of density, resulting in low uniformity and poor optical quality. The effect of injection speed was related to the switch-over point, which was found critical to the uniformity of the height. The optimal results were achieved when the polymer melts filled the mold cavity, or even a small excess when filling the cavity.

The ICM process parameters may also influence the replication as demonstrated in section 4.2. Hsien et al. [11] studied the effects of the process parameters on diffraction angle accuracy produced by IM and ICM and found that the most influential factors were different for each technology. For the IM, the mold temperature was the most influential factor with a contribution of 57.41%, followed by the melt temperature (19.23%) and the packing pressure (19.1%). For ICM, the compression speed was the most influential factor with a contribution of 55.7%, and the mold temperature was less important with a contribution of 4.02%.

To summarize, the most influential processing parameters referenced in the literature and their effect on replication degree are shown in Table 3.

7.2. Nanostructured functional coatings

As discussed in Section 5, the existence of AR coatings to reduce the reflection of the polymer surface plays an important role in the performance of lenses. Nevertheless, these AR coatings on top of polymeric substrates, typically formed using deposition methods, may lead to some issues as reported in previous sections, with a consequent decrease in the damage threshold limit of the lenses. Layered AR coatings are based on destructive interference at the layer interfaces (c.f. Section 5.1) and can reduce reflection up to several wavelengths at specific incident angles, which is characteristic of the intrinsic destructive interference mechanism.

Nature offers a possibility to circumvent this limitation. Moth-eye biomimetic nanostructures, as shown in Fig. 14 (a), first reported in the seminal work of Bernhard and Miller [168], show great promise in reducing surface Fresnel reflections and enhancing transmission over broad wavelength bands. Since then, a large number of nanostructured arrays have been developed as AR coatings or surfaces [169–171], which exhibit promising broadband and quasi-omnidirectional AR properties [172]. In practical applications, reducing the reflection and improving the transmission or absorption of light from wide angles of incidence in a broad wavelength range are crucial for improving the

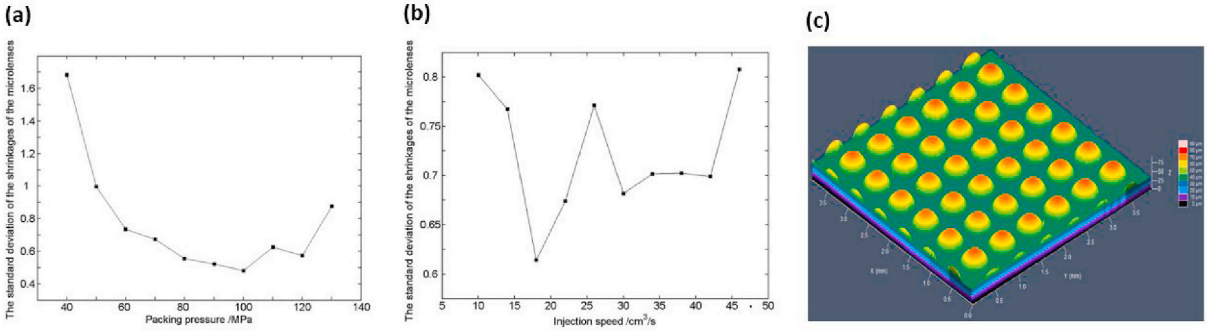

Fig. 13. Relation between the (a) packing pressure and (b) injection speed on the standard deviation of the shrinkages of the microlenses and (c) the 3D profile by laser scanning confocal microscope of the PMMA microlenses array molded with the optimized processing conditions. The results show that the microlenses maintain almost the same diameter, and the substrate exhibits almost no warpage, indicating the high accuracy achieved in the replication. Reprinted with permission from Ref. [161] Copyright © 2021, The Optical Society.

Table 3
Influence of processing parameters in the replication of microstructures.

Parameter	Technique	Effect in Replication of microstructures	Ref.
Mold temperature	IM, μ IM, μ ICM	The frozen layer is drastically reduced when the mold temperature is kept high during the filling	[156–160]
Melt Temperature	IM	The highest melt temperatures decrease viscosity in filling and significantly improve the replication	[162]
Injection speed	μ IM, IM	High injection speeds lead to high shear rates and heat convention, consequently, to a decrease in viscosity and preventing premature solidification. A high injection speed increases the cavity pressure, which drives the flow into the microstructures	[136,163]
Packing pressure	ICM, IM	Higher packing pressure allows higher replication degree	[156,160, 164]
Packing time	IM	The replication degree is directly proportional to the increase of packing time, achieving better results when the feature has a higher thickness	[164]
Compression gap	μ ICM	An increase in the compression gap reduces the transcription ratio of the microstructure. Should be kept as small as possible	[165]
Compression speed	ICM	High compression speed and high injection speed improved the replication by increasing the compression of the polymer melt and by homogenizing the cavity pressure distribution	[166]
Compression force	ICM	Compression force has a positive effect on replication degree, particularly in combination with high mold temperature	[165,167]

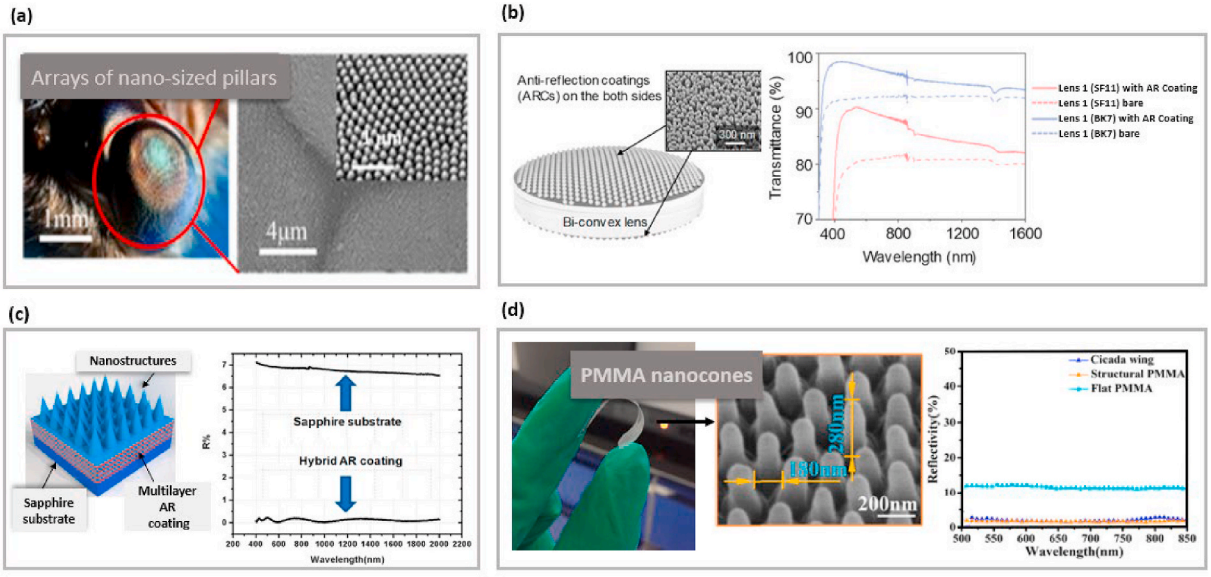

Fig. 14. Nanostructured AR coatings. (a) Moth eye (left) and the SEM image (right) showing the nanostructures on the outer surface of the corneal lens [179]; (b) Schematics of a bi-convex lens (left) with nanostructure AR coating on both sides. The SEM image shows the fabricated SiO2. Measured transmittance spectra (right) of optical lenses show that AR coatings improve the optical performance of the two lenses under study [169]; (c) Hybrid structure combining a multilayer optical coating with a SiO2 nanocone array on top to achieve the AR property (left). The measured reflectance of the hybrid coating is much lower than that measured for the bare sapphire substrate and close to zero (right) [171]; (d) Macroscopic view of the flexible PMMA film with nanocones mimicking Cicada wing (left image). SEM image of the side view of PMMA nanostructures 280 nm in height, 200 nm of pitch, and a gap of 180 nm between two structures (middle image). Comparison of the reflectivity measured for Cicada wing, nanostructured PMMA film, and the bare PMMA (Graph at the right-hand side) [170].

performance of optical devices. Nanostructured materials lead to tunable physicochemical properties, such as light absorption or color change, whereas a bulk material is limited to its inherent characteristics. Surfaces with micro and nanostructures are used in a broad range of optical applications, including microlenses, mirrors, photovoltaics, LEDs, photodetectors, and flat panel display applications [173–176].

In these applications, AR coatings are employed to minimize the reflection and enhance the absorption of light within the absorption wavelength band for nearly all incident directions, while improving the sensitivity and accuracy of the devices. For instance, Jang et al. [169] demonstrated that double-side AR coatings on bi-convex lenses increase the transmittance at a broadband wavelength from 300 to 1600, with better improvements for wavelengths ranging from 425 nm to 540 nm. The truncated cone-shaped SiO_2 nanostructures, applied to both sides of the optical lenses, were fabricated by first depositing a stack of SiO_2 and Ag on top of the lens. Then, a dewetting step followed by dry etching leads to the formation of the nanostructures. Two different types of lenses, namely BK7 and SF11 lenses, were employed with nanostructures having filling fractions between 60% and 80%, Fig. 14 (b). In addition, hybrid coatings combining nanostructures and multilayer optical coatings also demonstrated to significantly suppressed surface reflectance for a broad spectrum [171].

It is worth mentioning that nanostructured AR coatings have been implemented in different materials (c.f. Fig. 14). In particular, polymeric materials demonstrated great potential for creating broadband AR film. For instance, a flexible self-cleaning and broadband AR film, inspired by the cicada wing, has been successfully fabricated in PMMA [170], as presented in Fig. 14 (c). Experimental measurements show that the nanostructured PMMA film presents a similar reflectivity as the Cicada wing. Moreover, the average reflectivity of the structured PMMA film over the visible region was reduced from 10% to 2% when compared to a flat PMMA. Using a modified sol-gel process, it was possible to develop ordered nanocones arrays conferring a superhydrophobic surface on a flexible film. Many comprehensive reviews on nanostructured surfaces

with AR properties have been published in the literature [104,172]. In addition to optical applications, nanostructured surfaces are being used for example to create self-cleaning properties [177] and dry adhesion surfaces [178].

7.3. Fabrication of micro and nanostructures

As mentioned, the fabrication of micro and nanostructures by IM and its variants is achieved by considering the existence of these features machined on the surface of the mold or mold insert. Beyond the challenges in the process, the fabrication of optical mold insert is a crucial aspect to achieve high quality and replication, which is highly related to the final quality of the lens. The higher the quality of the mold insert, the better the quality of the replication [180]. Depending on dimension and surface requirements, fabrication technology and the material of the mold insert should be carefully selected.

The fabrication of optical mold inserts has been carried out using different technologies. Currently, the major challenge for most of the fabrication methods is to achieve optical surface quality with surface roughness <10 nm [75]. Table 4 shows the main techniques used to fabricate optical mold inserts over the past years in the production of molded lenses as well as a description of surface quality and form error. For a more complete description of fabrication technologies for optical mold inserts, the reader is referred to the work Roeder et al. [180].

Roeder et al. [192] reported that the remaining challenges in the fabrication of microstructured optics beyond the IM process, are i) structuring large areas, the current technologies tend to struggle when large areas are desired and long fabrication times are required, which becomes an economic disadvantage; ii) the metrology systems to evaluate the quality of the mold inserts as well as the replicated components are complex and requires a combination of different systems to the full evaluation and characterization of the components. Concerning material, inserts made of silicon are considered a good option due to the high-precision techniques that can be employed, namely conventional cleanroom technologies, typically used in the semiconductor and microfabrication industry [154]. However, the convenience of using silicon is limited by its delicate behavior when subjected to the high pressure encountered during IM processes. Other materials, such as metals, e.g. nickel [193], steel [194], and aluminum [195] are good candidates and they have also been studied.

8. Technologies to improve the injection molding

To improve the quality of high-precision optical lenses produced by IM, some technologies are elected due to their ability to increase replication and reduction of residual stress. According to the literature, the most referenced is the variotherm system, which allows rapid mold heating and cooling, then vacuum-assisted microinjection molding used to increase the replication, and more recently, the conformal cooling channel to reduce thermally-induced residual stress.

8.1. Vacuum-assisted micro injection molding

The vacuum venting has been implemented as an auxiliary molding technology in the μ IM process to improve the filling due to high values of injection speed and the fact of surface roughness is more critical at the microscale and air traps are more susceptible. With the increase in roughness, the advance of melt flow is not homogenous due to difficulties to filling the irregular surface and therefore originating the air trap. The heat transfer from melt to the mold is also slowed down due to the contact surface reduction and consequently the viscosity increases [196]. A vacuum venting may reduce this effect and allow the removal of trapped air within the microstructures of the insert, responsible for the incomplete filling. Therefore, it is possible to enhance the replication and accuracy [162].

Sorgato and Lucchetta [162] observed that a combination of high mold temperature and air evacuation could be successfully applied to increase the average height of the microstructures, especially for low viscosity material. The interactions between air evacuation and other factors suggested that a combination of low-viscosity and low-wetting properties could be the ideal conditions. Additionally, the study showed that the venting conditions are not as important as the mold temperature, stating that the vacuum conditions only could increase the height of the microstructures by 17%, while an increase in mold temperature represented a gain of approximately 107%. In literature, it was reported that air evacuation has a different effect on polymers. Sorgato et al. [197] studied the effect of air evacuation on COC and PS and reported that air evacuation was more influential in COC, with an increment of replication by 13.6%, while for PS the variation was not significant. This behavior is explained due to a higher wettability of COC who led to higher interfacial interactions that resulted in a better replication when molding this polymer after air evacuation. Without vacuum venting the COC replication decreased due to the presence of air counteracts the beneficial effect of COC wettability. Recently, Sorgato et al. [163], concluded that applying vacuum venting could reduce pressure and melt temperature and may, in turn, counteract the benefits of air evacuation to filling the microstructures. In fact, in the study, the melt temperature was reported to be reduced by 7% when the vacuum is employed. It was also concluded that vacuum venting could improve replication but needs careful process optimization.

On other hand, some studies do not agree with the application of vacuum venting to enhance replication and affirm that their effect on replication is not significant. For instance, Sortino et al. [74] showed that vacuum IM implies an increase in cycle time due to the time needed to reach the vacuum condition inside the cavity, in comparison with IM and ICM, which makes it a disadvantage in industrial application. In addition. Chen et al. [198] evaluated the accuracy of features with 30–50 μm width and with 120 and 600 μm depth, in molded PMMA parts. In this study, was proven application of vacuum may improve the replication degree, however, the effect is negligible at high mold temperatures, i.e. above 120 °C. When a mold temperature of 140 °C was

Table 4
Overview of the manufacturing technologies for optical mold inserts, typical achieved dimensions, and surface quality reported in the literature.

Fabrication Technologies	Surface roughness	Form error	Structure dimensions	Application	Ref.
Photolithography	<5 nm	–	<100 nm	DVD pickup lens	[11,60,181];
Ultraprecision milling	<10 nm	<40 nm	4 μm	Microlenses array	[75];
LIGA[a]	<10 nm	–	<1 μm	Microlenses array	[182–184]
Ultraprecision diamond machine	<40 nm	0.2 μm	10 μm	Micro Alvarez lenses array	[185];
Slow Slide Servo	<10 nm	50 μm	5 μm	Microlenses array Eye lenses	[186,187];
Ultra-precision diamond ball-end milling	<30 nm	0.5 μm	45 μm	Microlenses array	[57]
Diamond turning	<8 nm	<300 nm	5 μm	Aspheric lenses Fresnel lenses	[188];
Diamond Milling	<10 nm	25 nm	50 μm	Aspheric surfaces on lenses	[189]
Electrical discharge machining (EDM)	<0.1 μm	2 μm	<10 μm	Lenses array	[190]
Nanoimprinting using anodic porous alumina molds	–	–	<300 nm	Lenses with an AR structure	[191]

[a] LIGA: German acronym for Lithographie, Galvanoformung, Abformung (Lithography, Electroplating, and Molding).

used, a slight improvement of approximately 1% was verified. Sha et al. [152] observed a negative effect of vacuum venting on the replication. It was explained that the air evacuation could lead to a decrease in the mold temperature, as a result of removing warm air from the cavity, mainly for polymers that are sensitive to changes of temperature, such as polystyrene. The effect of the air evacuation, in a study carried out by Luchetta et al. [160], also resulted in a reduction in the average height of the microfeatures by 16%. The same explanation was given, a decrease of the surface temperature as a result of the warm air removal caused a reduction of replication.

8.2. Variotherm system

The mold temperature is an important parameter in the source of residual stress and the replication degree. Many authors have been studying the influence of these parameters over the years. A consensus has been reached in the research community: an elevated mold temperature is a necessity to successfully replicate the micro and nanostructures, particularly with high aspect ratios [57,199]. A solution to control the mold temperature is to use a dynamic temperature control system, known as the variotherm system. The process is illustrated in Fig. 15 (b) and is compared with conventional IM, e.g. without dynamic temperature control system, Fig. 15 (a).

This system has been used mostly to reduce or eliminate weld lines and to enhance the superficial gloss [200,201]. More recently, it was proved to be indispensable in the field of precision optical lenses manufacturing, being reported a reduction of residual stress and increase in uniformity by 88% when the warm circuit is increased by 84% [135,202]. The process allows the heating of the mold cavity, at a temperature higher than the T_g of the polymer. Thus, it is possible to avoid premature freezing of melt when it comes in contact with the mold wall. Through this process, the frozen layer formed during filling, which is the main cause of residual stress [38], is reduced or eliminated. The mold temperature increases, typically about 20 °C or 30 °C degrees higher than the T_g during filling and packing. The viscosity of the material and the flow resistance are reduced, and the melt polymer fills the cavity more easily and rapidly. This phenomenon avoids the hesitation effect of the melt flow in the entrance of microstructures, as explained in Fig. 16. This is considered the major benefit of using the variotherm system in the replication process. The variotherm system also allows a stress birefringence reduction since the frozen layer is eliminated [203, 204].

After the filling and packing stage, the part is cooled and the temperature is reduced below the heat deflection temperature of the polymer and finally, the part is ejected. According to Zhang et al. [205], the temperature must not be excessively higher during filling, since it may cause adhesion between the melt polymer and the metal walls of the mold. In the presence of microstructures, they may be damaged. The heating stage may be accomplished with different methods. These methods are differentiated by their effectiveness and heat transfer that allows rapid heating and cooling. There are methods of heating through electric energy, consisting of transforming electric energy into thermal energy, radiation [203], induction [206,207], and heating rods [208]. There are other methods, which use heat transfer by convection water [209], steam [210], oil [211], or hot gas [212].

In literature, several authors have been studying the improvement of birefringence using a dynamic mold temperature control. Chen et al. [213] studied the use of rapid heating and cooling in μ IM of PC and reported that when mold temperature achieves $265°C$, which is the material melt temperature, the birefringence pattern was almost eliminated. Park et al. [214] studied the effect of rapid mold heating in the birefringence distribution. The authors found that the increase in the mold temperature reduces the maximum and average birefringence, up to 50%. This decrease is most significant when the mold temperature is above T_g, thus reducing the molecular orientation induced by flow and consequently anisotropy. More recently, Hong et al. [215] studied the effect of a dynamic temperature control system combined with ICM in replication degree and birefringence. In this research, the system was implemented with steam. It was shown a high replication degree when the dynamic temperature control system was used. Furthermore, combining the two mentioned techniques enabled the replication degree to be increased to 20% with a mold temperature below the T_g. In other words, it was shown that with the combination of these two techniques is possible to have a successful filling of the microstructures with a lower temperature than when it only uses dynamic temperature control system.

Zhang et al. [135] studied the precision replication of the microlenses arrays, with a height smaller than 200 μm, and the optical retardation. It was analyzed the use of variotherm, for that it was adopted a system with a valve switch between warm and cool circuits. The best results of surface quality and geometric accuracy, i.e. PV of form error, are obtained when switching from warm to cold immediately after the end of the packing, Fig. 17 (a), and the residual stress was reduced with the delay of the warm-cold switch conditions, Fig. 17 (b). When the warm circuit was higher than the T_g of the polymer, a combination of uniformly low residual stress with satisfying surface quality and geometric accuracy was achieved, Fig. 17 (c) and (d). Furthermore, it was observed that the quality of stress birefringence was influenced also by the screw movements, the cavity pressure, the temperature, and the relaxation of the molecular orientations. In conclusion, variotherm control of the mold temperature ensures the reduction of the residual stresses, while achieving excellent surface quality and geometric accuracy.

In addition to the traditional methods mentioned above, some re-

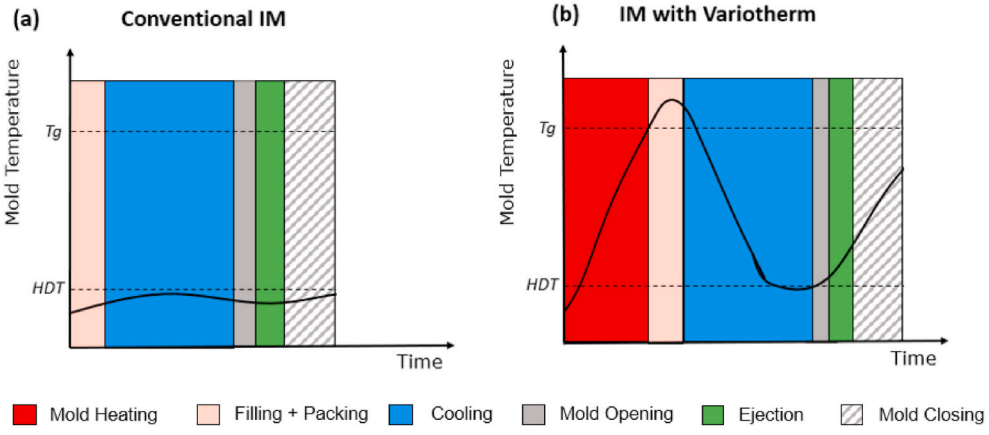

Fig. 15. Cycle comparison of (a) conventional IM and (b) IM with variotherm.

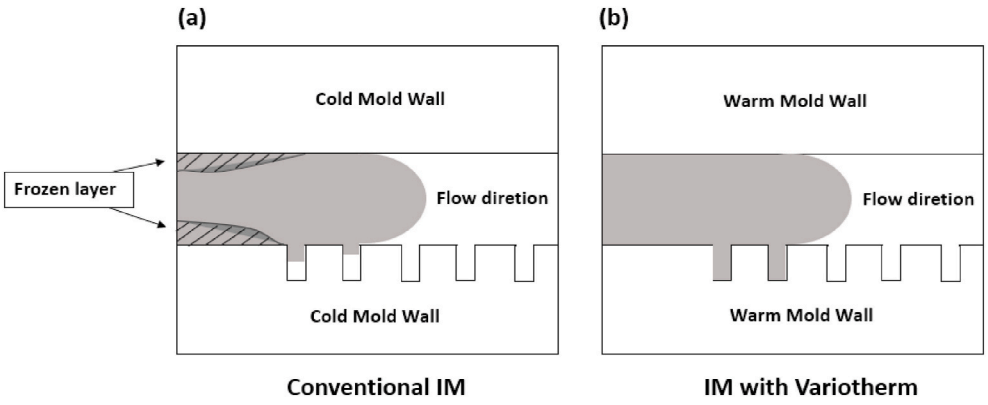

Fig. 16. Comparison of the flow hesitation effect at the entrance of the microstructures in filling step in (a) conventional IM and (b) IM with variotherm.

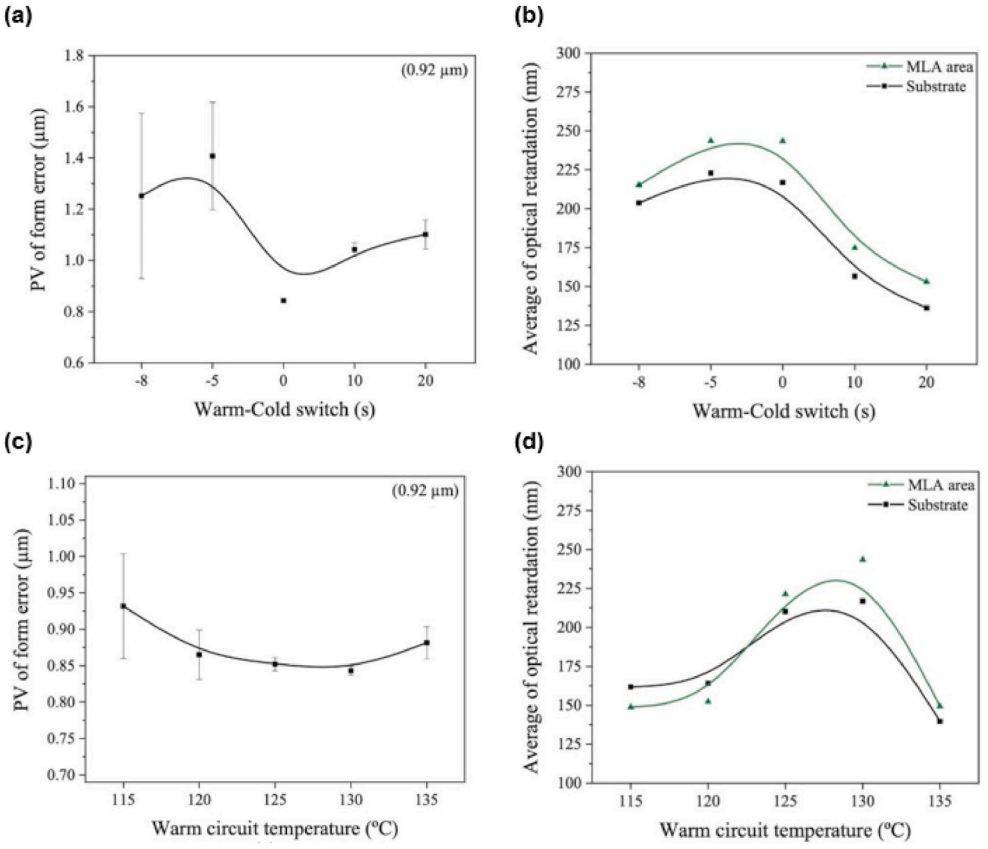

Fig. 17. Effect of warm-cold switch and effect of the warm circuit on (a), (c) geometric accuracy, peak-to-valley (PV) of form error (corresponding values of the mold insert of 0.92 μm) respectively; Effect of warm-cold switch and effect of the warm circuit on (b), (d) optical retardation, respectively [135].

searchers developed new methods. To increase the replication and the appearance of molding parts, Luchetta et al. [216] developed an innovative technology for rapid heating and cooling based on mold inserts made of open-cell aluminum foam. The thermal behavior of the system was modeled to verify if the metallic foam inserts largely increased the heat exchange rate and compared to conventional cooling channels. The experimental results showed a significant improvement in the replication degree, increasing the replication from 45 to 120 µm, especially for those features characterized by the smallest values of thickness and aspect ratio. Chen et al. [217] investigated the use of gas-assisted heating for mold surfaces and it was shown that the efficiency compared with other temperature control methods was improved. The result indicates the great potential of gas-assisted heating in µ IM to achieve high replication accuracy with a minimum cycle time increase. The average replication accuracy in the PC part was improved 89% and 95%, at mold temperatures of 130 °C and 150 °C, respectively. The results show high accuracy, of 99.8% for a mold temperature of 150 °C, and an improvement of 21.4% over conventional IM was achieved.

8.3. *Conformal cooling channels*

More recently, with the development of additive manufacturing technology, the integration of conformal cooling channels has been pointed out as the most promising solution to reduce thermal-induced residual stress caused by unbalanced cooling. This new trend in the production of optical lenses allows to improve the geometric accuracy, reduce warpage and deformations in optical lenses. Large-diameter [218] and high thickness polymer lenses [219] play a substantial role

in the optical industry and are more susceptible to slower and unbalanced cooling.

Conformal cooling, when compared to conventional cooling channels, has more benefits, such as, the reduction of cycle time, which may be an economic advantage in high-production rates [220,221], higher cooling efficiency, and superior temperature distribution in the mold cavity, consequently reducing thermally-induced warpage [222]. The use of additive manufacturing techniques enables the production of complex geometries through hybrid manufacturing processes, which combine metallic powder-based laser additive processes and subtractive machining processes [223]. The possibility of manufacturing complexity 3D features enables the production of complex cooling channels, capable of following the cavity of the geometry, improving the uniformity of cooling, and providing a higher heat transfer over conventional cooling.

The system and method for conformal cooling during a lens manufacturing process [224] have been patented. Through finite element simulation of the production of contact lenses, Lin et al. [8] demonstrated a cycle reduction of about 20% with the addition of the conformal cooling channel. In addition, Chung [225] combined finite element analysis with a gradient-based algorithm and a robust genetic algorithm to determine the optimum layout of cooling channels. It was shown that a robust genetic algorithm optimized conformal cooling channel had the highest cooling efficiency and superior melt front temperature distribution in the mold cavity, thus reducing thermally-induced warpage. In general, according to the simulation results, the use of conformal cooling channels reduced, in both algorithms studied, the surface temperature difference of the melt, the cycle time, and warpage compared to the conventional cooling channel.

9. Conclusions remarks

High mass production of high-precision optical lenses is a challenge for the industry. With the sudden development of the self-driving, electronic, photovoltaic, and medical industries, the demand for high-quality optical components has shown a growing trend. Polymers demonstrate numerous benefits in optics. They enable mass production with relatively low cost, high automation, short cycle time compared to glass, and satisfactory replication accuracy. A comprehensive review of prior works provides an opportunity to describe the main materials and technologies used to produce high-precision polymer optical lenses. The main features of the different materials and technologies, the advantages, and their main challenges were presented in this review.

The ICM has been elected as the best technology to produce high-precision optical lenses. Moreover, the final quality of the optical lens was proven that be strongly dependent on process parameters and requires high control over them. The majority of the studies were focused on the optimization of the process conditions, experimentally and through numerical simulation. It was concluded that numerical simulations are a cost-effective way to optimize the process and final optical properties. Furthermore, the influence of the gate and the runner was also addressed, as well as the review of additional systems which may be incorporated in the mold and demonstrated a beneficial increment in the replication and reduction of residual stress. The recent advances in this area, the benefits in optical performance, and the replication of the microstructures were overviewed and discussed. Additionally, in the field of optimization of the process parameters, a recent approach has emerged as a new trend with the potential to achieve optimal quality. Applying ANNs to predict the optimal process parameters of the IM process enables you to quickly obtain the optimal processing parameters according to the required quality of the optical lenses, for instance, accuracy and geometric deviations. Furthermore, it was given a brief overview of the functional coatings, such as AR coatings, with recent advances in this field, and its application on optical lenses.

It is important to highlight that, with increasing requirements of the optical components, such as accuracy, the reduced structure dimensions, and the high surface quality, the development of high-performance tools, using new materials, and new cost-effective technologies for the micro and nanofabrication of optical inserts will be even more significant in the future. Further developments in the optical field, such as the integration of high quality mold inserts, accurate replication processes, and precise micro-assembly methods will offer new opportunities and applications for optical polymers, enabling performance improvement, lightweight systems, new complex surface forms with desirable freedom of design and miniaturization. Achieving high-performance optical coatings on these complex surface forms demands the constant development of thin-film fabrication technologies. Furthermore, aspects as cost-efficiency, environmental impact, and coating system durability have to be considered.

Even though the polymer optical lenses have been explored, as outlined in this review, the continuous improvements and optimization of the process with the developments of new lens designs and in novel applications, appear to have countless potential in future research in different scientific fields.

Funding

This work was supported by European Regional Development Fund (ERDF), through the Competitiveness and Internationalization Operational Program (COMPETE 2020) of the Portugal 2020 Program [SMART4CAR- Smart Surfaces for Automotive Components - POCI-01-0247-FEDER- 045096].

Declaration of competing interest

The authors declare that they have no known competing financial interests or personal relationships that could have appeared to influence the work reported in this paper.

References

[1] Terefe N. Transmitter lens for a lidar based sensor. In: European Patent. EP 3 054 313 A1; 2016.
[2] Ding Y, Liu X, Zheng Z, Gu P. Freeform LED lens for uniform illumination. Opt Express 2018;16:12958–66. https://doi.org/10.1364/oe.16.012958.
[3] Qandil H, Wang S, Zhao W. Application-based design of the fresnel-lens solar concentrator. Renew. Wind Water Sol. 2019;6:4861–9. https://doi.org/10.1186/s40807-019-0057-8.
[4] Lee SW, Joh HH, Hong JS, Lyu MY. Birefringent analysis of plastic lens injection molding for mobile phone camera. Trans. Mater. Process. 2011;20:54–9. https://doi.org/10.5228/kstp.2011.20.1.54.
[5] Lee HS, Jeon WT, Kim SW. Development of plastic lenses for high-resolution phone camera by injection-compression molding. Trans. Korean Soc. Mech. Eng. A 2013;37:39–46. https://doi.org/10.3795/KSME-A.2013.37.1.039.
[6] Heiney AJ, Jiang CL, Reysen WH. Polymer molded lenses for optoelectronics. In: Proc - Electron Components Technol Conf. 170–6; 1995. https://doi.org/10.1109/ectc.1995.514379.
[7] Milster TD, Upton HL. Objective lens design for multiple-layer optical data storage. In: Opt Data Storage Top Meet ODS Conf Dig; 1997. https://doi.org/10.1109/ODS.1997.606130.
[8] Lin YF, Wu JR, Liu BH, Wei WCJ, Wang AB, Luo RC. Improved contact lens injection molding production by 3D printed conformal cooling channels. In: SII 2017 - 2017 IEEE/SICE Int Symp Syst Integr; 2018. p. 89–94. https://doi.org/10.1109/SII.2017.8279194. 2018-Janua.
[9] La M, Park SM, Kim W, Lee C, Kim C, Kim DS. Injection molded plastic lens for relay lens system and optical imaging probe. Int J Precis Eng Manuf 2015;16:1801–8. https://doi.org/10.1007/s12541-015-0235-6.
[10] Michaeli W, Walach P. Optical plastics components: replication processes and plastic materials. In: Brinksmeier E, Riemer O, RalfGläbe, editors. Fabrication of complex optical components: from mold design to product. first ed. Springer Verlag; 2012. p. 25–40. https://doi.org/10.1007/978-3-642-33001-8.
[11] Wu CH, Chen WS. Injection molding and injection compression molding of three-beam grating of DVD pickup lens. Sens Actuat A Phys 2006;125:367–75. https://doi.org/10.1016/j.sna.2005.07.025.
[12] Michaeli W, Hessner S, Klaiber F. Analysis of different compression-molding techniques regarding the quality of optical lenses. J Vac Sci Technol B Microelectron Nanom Struct 2009;27:1442. https://doi.org/10.1116/1.3079765.
[13] Pazos M, Baselga J, Bravo J. Limiting thickness estimation in polycarbonate lenses injection using CAE tools. J Mater Process Technol 2003;143–144:438–41. https://doi.org/10.1016/S0924-0136(03)00425-.
[14] Okagbare PI, Emory JM, Datta P, Goettert J, Soper SA. Fabrication of a cyclic olefin copolymer planar waveguide embedded in a multi-channel poly(methyl

methacrylate) fluidic chip for evanescence excitation. Lab Chip 2010;10:66–73. https://doi.org/10.1039/b908759a.
[15] Chang YJ, Yu CK, Chiu H, Sen, Yang WH, Lai HE, Wang PJ. Simulations and verifications of true 3D optical parts by injection molding process. In: 67th Annual technical conference of the Society of plastics Engineers 2009, 22-24 June 2009, Chicago, Illinois, USA, vol. 1. ANTEC; 2009. 253–8.
[16] Minami K. Optical plastics. In: Bäumer S, editor. Handbook of plastics optics. second ed. Germany: Wiley-VCH Verlag GmbH & Co; 2010. p. 123–60.
[17] Schulz U, Schallenberg UB, Kaiser N. Antireflection coating design for plastic optics. Appl Opt 2002;41:3107–10. https://doi.org/10.1364/AO.41.003107.
[18] Paul P, Pfeiffer K, Szeghalmi A. Antireflection coating on PMMA substrates by atomic layer deposition. Coatings 2020;10:1–13. https://doi.org/10.3390/coatings10010064.
[19] Charitidis C, Laskarakis A, Kassavetis S, Gravalidis C, Logothetidis S. Optical and nanomechanical study of anti-scratch layers on polycarbonate lenses. Superlattice Microst 2004;36:171–9. https://doi.org/10.1016/j.spmi.2004.08.015.
[20] Zhou G, He J, Xu L. Antifogging antireflective coatings on Fresnel lenses by integrating solid and mesoporous silica nanoparticles. Microporous Mesoporous Mater 2013;176:41–7. https://doi.org/10.1016/j.micromeso.2013.03.038.
[21] Chang YR, Chiu H, Sen, Yang WH, Chang RY. A novel approach for predicting birefringence of optical parts. In: ANTEC 2007 Plastics: Annual Technical Conference Proceedings. 4; 2007. p. 2476–9.
[22] Isayev AI. Orientation development in the injection molding of amorphous polymers. Soc Plast Eng Inc 1983;23:271–84. https://doi.org/10.1002/pen.760230507.
[23] Tsai KM. Runner design to improve quality of plastic optical lens. Int J Adv Manuf Technol 2013;66:523–36. https://doi.org/10.1007/s00170-012-4346-2.
[24] Tsai KM, Hsieh CY, Lo WC. A study of the effects of process parameters for injection molding on surface quality of optical lenses. J Mater Process Technol 2009;209:3469–77. https://doi.org/10.1016/j.jmatprotec.2008.08.006.
[25] Liu J, Chen X, Lin Z, Diao S. Multiobjective optimization of injection molding process parameters for the precision manufacturing of plastic optical lens. Math Probl Eng 2017:1–13. https://doi.org/10.1155/2017/2834013Research.
[26] Lai HE, Wang PJ. Study of process parameters on optical qualities for injection-molded plastic lenses. Appl Opt 2008;47. https://doi.org/10.1364/AO.47.002017. 2017–27.
[27] Bensingh RJ, Boopathy SR, Jebaraj C. Minimization of variation in volumetric shrinkage and deflection on injection molding of Bi-aspheric lens using numerical simulation. J Mech Sci Technol 2016;30:5143–52. https://doi.org/10.1007/s12206-016-1032-6.
[28] Lin CM, Hsieh HK. Processing optimization of Fresnel lenses manufacturing in the injection molding considering birefringence effect. Microsyst Technol 2017;23:5689–95. https://doi.org/10.1007/s00542-017-3375-z.
[29] Chen SC, Chen YC, Peng HS, Huang LT. Simulation of injection-compression molding process, Part 3: effect of process conditions on part birefringence. Adv Polym Technol 2002;21:177–87. https://doi.org/10.1002/adv.10024.
[30] Lin CM, Chen WC. Optimization of injection-molding processing conditions for plastic double-convex Fresnel lens using grey-based Taguchi method. Microsyst Technol 2020;26:2575–88. https://doi.org/10.1007/s00542-020-04798-6.
[31] Chipman RA, Lam W-ST, Young G. Stress-induced birefringence. Polarized light and optical systems. first ed. CRC Press Taylo & Francis Group; 2019. p. 879–907.
[32] Tagaya A. Birefringence of polymer. Encycl Polym Nanomater 2013;116:1–6. https://doi.org/10.1007/978-3-642-36199-9.
[33] Narasimhamurty TS. Photoelastic and Electo-optic properties of Crystals. first ed. New York Inc., United States: Springer-Verlag; 1981.
[34] Macías C, Meza O, Pérez E. Relaxation of residual stresses in plastic cover lenses with applications in the injection molding process. Eng Fail Anal 2015;57:490–8. https://doi.org/10.1016/j.engfailanal.2015.07.026.
[35] Weng C, Lee WB, To S. Birefringence techniques for the characterization of residual stresses in injection-moulded micro-lens arrays. Polym Test 2009;28:709–14. https://doi.org/10.1016/j.polymertesting.2009.06.007.
[36] Weng C, Lee WB, To S, Jiang B yan. Numerical simulation of residual stress and birefringence in the precision injection molding of plastic microlens arrays. Int Commun Heat Mass Tran 2009;36:213–9. https://doi.org/10.1016/j.icheatmasstransfer.2008.11.002.
[37] Chen Y-C, Nian S-C, Huang M-S. Optical design of the Fresnel lens for LED-driven flashlight. Appl Opt 2016;55:712. https://doi.org/10.1364/ao.55.000712.
[38] Fang F, Zhang N, Zhang X. Precision injection molding of freeform optics. Adv Opt Technol 2016;5:303–24. https://doi.org/10.1515/aot-2016-0033.
[39] Kim D, Chang S, Kwon HS. Wide field-of-view, high-resolution plastic lens design with low f-Number for disposable endoscopy. Photonics 2021;8. https://doi.org/10.3390/photonics8040089.
[40] Bashir Khan S, Wu H, Pan C, Zhang Z. A mini review: antireflective coatings processing techniques, applications and future perspective. Res Rev J Mater Sci 2017;5:36–54. https://doi.org/10.4172/2321-6212.1000192.
[41] Charitidis C, Laskarakis A, Kassavetis S, Gravalidis C, Logothetidis S. Optical and nanomechanical study of anti-scratch layers on polycarbonate lenses. Superlattice Microst 2004;36:171–9. https://doi.org/10.1016/j.spmi.2004.08.015.
[42] Sethi SK, Manik G. Recent progress in super hydrophobic/hydrophilic self-cleaning surfaces for various industrial applications: a review. Polym Plast Technol Eng 2018;57:1932–52. https://doi.org/10.1080/03602559.2018.1447128.
[43] Ganesh VA, Raut HK, Nair AS, Ramakrishna S. A review on self-cleaning coatings. J Mater Chem 2011;21:16304. https://doi.org/10.1039/c1jm12523k.
[44] Pijpers AP, Meier RJ. Adhesion behaviour of polypropylenes after flame treatment determined by XPS(ESCA) spectral analysis. J Electron Spectrosc Relat Phenom 2001;121:299–313.
[45] Dubreuil MF, Bongaers EM. Use of atmospheric pressure plasma technology for durable hydrophilicity enhancement of polymeric substrates. Surf Coating Technol 2008;202:5036–42.
[46] Lappschies M, Schallenberg U, Jakobs S. Exclusive examples of highperformance thin-film optical filters for fluorescence spectroscopy made by plasma-assisted reactive magnetron sputtering. SPIE 8168. Adv Opt Thin Film 2011;IV:8. https://doi.org/10.1117/12.896846. 81680Y.
[47] Lappschies M, Weber T, Venancio LM, Jakobs S. Advanced dielectric coatings for the Euclid mission telescope manufactured by the PARMS process. In: Opt Interf Coatings 2016, OSA Tech Dig; 2016.
[48] Razskazovskaya O, Krausz F, Pervak V. Multilayer coatings for femto- and attosecond technology. Optica 2017;4:1–129.
[49] World's Foremost optical polymer for precision-molded optics. Zeon Corporation n.d. https://www.zeonex.com/optics.aspx.html#techdata. [Accessed 19 April 2021].
[50] SCHOTT Advanced Optics. Schott N-BK7®. n.d. https://shop.schott.com/advanced_optics/en/Optical-Glass/SCHOTT-N-BK7/c/optical-glass/glass-SCHOTTN-BK7®. [Accessed 19 April 2021].
[51] Gillen GD, DiRocco C, Powers P, Guha S. Temperature-dependent refractive index measurements of wafer-shaped InAs and InSb. Appl Opt 2008;47:164–8. https://doi.org/10.1364/AO.47.000164.
[52] Beich WS, Turner N. Polymer optics: a manufacturer's perspective on the factors that contribute to successful programs. In: Krevor DH, Beich WS, editors. Polym. Opt. Des. Fabr. Mater., vol. 7788. Proc. of SPIE; 2010. https://doi.org/10.1117/12.861364. 778805–1.
[53] Kohara T. Development of new cyclic olefin polymers for optical uses. Macromol Symp 1996;101:571–9. https://doi.org/10.1002/masy.19961010163.
[54] Nunes PS, Ohlsson PD, Ordeig O, Kutter JP. Cyclic olefin polymers: emerging materials for lab-on-a-chip applications. Microfluid Nanofluidics 2010;9:145–61. https://doi.org/10.1007/s10404-010-0605-4.
[55] Mayer R. Precision injection molding: how to make polymer optics for high volume and high precision applications. Opt Photonik 2007;2:46–51. https://doi.org/10.1002/opph.201190286.
[56] Kalima V, Pietarinen J, Siitonen S, Immonen J, Suvanto M, Kuittinen M, et al. Transparent thermoplastics: replication of diffractive optical elements using micro-injection molding. Opt Mater 2007;30:285–91. https://doi.org/10.1016/j.optmat.2006.11.046.
[57] Kirchberg S, Chen L, Xie L, Ziegmann G, Jiang B, Rickens K, et al. Replication of precise polymeric microlens arrays combining ultra-precision diamond ball-end milling and micro injection molding. Microsyst Technol 2012;18:459–65. https://doi.org/10.1007/s00542-011-1414-8.
[58] Holthusen AK, Riemer O, Schmütz J, Meier A. Mold machining and injection molding of diffractive microstructures. J Manuf Process 2017;26:290–4. https://doi.org/10.1016/j.jmapro.2017.02.014.
[59] Loaldi D, Quagliotti D, Calaon M, Parenti P, Annoni M, Tosello G. Manufacturing signatures of injection molding and injection compression molding for micro-structured polymer fresnel lens production. Micromachines 2018;9. https://doi.org/10.3390/mi9120653.
[60] Luo C-W, Chiang Y-C, Cheng H-C, Wu C-Z, Huang C-F, Wu C-W, et al. A novel and rapid fabrication for microlens arrays using microinjection molding. Polym Eng Sci 2011;51:391–402. https://doi.org/10.1002/pen.21840.
[61] Osswald T. Injection molding. Underst. Polym. Process. Process. Gov. Equations. second ed. Munich: Hanser Publishers; 2017. 199–145.
[62] Roeder M, Schilling P, Hera D, Guenther T, Zimmermann A. Influences on the fabrication of diffractive optical elements by injection compression molding. J Manuf Mater Process 2018;2:5. https://doi.org/10.3390/jmmp2010005.
[63] Zoetelief WF, Douven LFA, Ingen Housz AJ. Residual thermal stresses in injection molded products. Polym Eng Sci 1996;36:1886–96. https://doi.org/10.1002/pen.10585.
[64] Young W Bin. Residual stress induced by solidification of thermoviscoelastic melts in the postfilling stage. J Mater Process Technol 2004;145:317–24. https://doi.org/10.1016/j.jmatprotec.2003.07.015.
[65] Guevara-Morales A, Figueroa-López U. Residual stresses in injection molded products. J Mater Sci 2014;49:4399–415. https://doi.org/10.1007/s10853-014-8170-y.
[66] Flaman AAM. Buildup and relaxation of molecular orientation in injection molding. Part II: experimental verification. Polym Eng Sci 1993;33:202–10. https://doi.org/10.1002/pen.760330403.
[67] Kabanemi K, Vaillancourt H, Wang H, Salloum G. Residual stresses, shrinkage, and warpage of complex injection molded products : numerical simulation and experimental validation. Polym Eng Sci 1998;38:21–37. https://doi.org/10.1002/pen.760330403.
[68] Lin CM, Chen YW. Grey optimization of injection molding processing of plastic optical lens based on joint consideration of aberration and birefringence effects. Microsyst Technol 2019;25:621–31. https://doi.org/10.1007/s00542-018-4001-4.
[69] Wang P, Lai H. Study of residual birefringence in injection molded lenses (2007). In: SPE ANTEC Conf; 2007. p. 2498.
[70] Loaldi D, Calaon M, Quagliotti D, Parenti P, Annoni M, Tosello G. Tolerance verification of precision injection moulded Fresnel lenses. Procedia CIRP 2018;75:137–42. https://doi.org/10.1016/j.procir.2018.05.004.

[71] Wu CH, Su Y-L. Optimization of wedge-shaped parts for injection molding and injection compression molding. Int Commun Heat Mass Tran 2003;30:215–24. https://doi.org/10.1016/S0735-1933(03)00032-0.

[72] Michaeli W, Wielpuetz M. Optimization of the optical part quality of polymer glasses in the injection compression moulding process. Macromol Mater Eng 2000;284–285:8–13. https://doi.org/10.1002/1439-2054(20001201)284. 1<8::AID-MAME8>3.0.CO;2-1.

[73] Michaeli W, Heßner S, Klaiber F, Forster J. Geometrical accuracy and optical performance of injection moulded and injection-compression moulded plastic parts. CIRP Ann - Manuf Technol 2007;56:545–8. https://doi.org/10.1016/j.cirp.2007.05.130.

[74] Sortino M, Totis G, Kuljanic E. Comparison of injection molding technologies for the production of micro-optical devices. Procedia Eng 2014;69:1296–305. https://doi.org/10.1016/j.proeng.2014.03.122.

[75] Roeder M, Drexler M, Rothermel T, Meissner T, Guenther T, Zimmermann A. Injection compression molded microlens arrays for hyperspectral imaging. Micromachines 2018;9:1–14. https://doi.org/10.3390/mi9070355.

[76] Chen SC, Chen YC, Peng HSHU. Simulation of injection – compression-molding process. II. Influence of process characteristics on Part Shrinkage. J Appl Polym Sci 2000;75:1640–54. https://doi.org/10.1002/(SICI)1097-4628(20000328)75.13<1640::AID-APP10>3.0.CO;2-L.

[77] Young W Bin. Effect of process parameters on injection compression molding of pickup lens. Appl Math Model 2005;29:955–71. https://doi.org/10.1016/j.apm.2005.02.004.

[78] Chen S, Li B, Zhang Y, Jin Z. Effects of the injection compression process parameters on residual stress of plastic lenses. Appl Opt 2020;59:9626–32. https://doi.org/10.1364/AO.404024.

[79] Lo WC, Tsai KM, Hsieh CY. Six Sigma approach to improve surface precision of optical lenses in the injection-molding process. Int J Adv Manuf Technol 2009;41:885–96. https://doi.org/10.1007/s00170-008-1543-0.

[80] Spina R, Walach P, Schild J, Hopmann C. Analysis of lens manufacturing with injection molding. Int J Precis Eng Manuf 2012;13:2087–95. https://doi.org/10.1007/s12541-012-0276-z.

[81] Hu GH, Cui ZS. Effect of packing parameters and gate size on shrinkage of aspheric lens parts. J Shanghai Jiao Tong Univ (Sci) 2010;15:84–7. https://doi.org/10.1007/s12204-010-7176-0.

[82] Lu X, Khim LS. A statistical experimental study of the injection molding of optical lenses. J Mater Process Technol 2001;113:189–95. https://doi.org/10.1016/S0924-0136(01)00606-9.

[83] Shieh JY, Wang LK, Ke SY. A feasible injection molding technique for the manufacturing of large diameter aspheric plastic lenses. Opt Rev 2010;17:399–403. https://doi.org/10.1007/s10043-010-0074-8.

[84] Yin X-H, Yang C, Li X-P, Liang D, Zhang Z-H, Tang Y, et al. 3D thickness distributions of plano lenses as a means of cavity pressure characterization in microinjection molding. Opt Express 2018;26:11250. https://doi.org/10.1364/oe.26.011250.

[85] Jialing W, Pengfei W. Simulation and optimization of aspheric plastic lens injection molding. J Wuhan Univ Technol -Materials Sci Ed 2005;20:86–9. https://doi.org/10.1007/BF02838498.

[86] Zhang H, Zhang N, Han W. Characterization of process and machine dynamics on the precision replication of microlens arrays using microinjection moulding. Adv Manuf 2021. https://doi.org/10.1007/s40436-020-00341-y.

[87] Bensingh RJ, Machavaram R, Boopathy SR, Jebaraj C. Injection molding process optimization of a bi-aspheric lens using hybrid artificial neural networks (ANNs) and particle swarm optimization (PSO). Meas J Int Meas Confed 2019;134:359–74. https://doi.org/10.1016/j.measurement.2018.10.066.

[88] Tsai KM, Luo HJ. An inverse model for injection molding of optical lens using artificial neural network coupled with genetic algorithm. J Intell Manuf 2017;28:473–87. https://doi.org/10.1007/s10845-014-0999-z.

[89] Yang C, Su L, Huang C, Huang H-X, Castro JM, Yi AY. Effect of packing pressure on refractive index variation in injection molding of precision plastic optical lens. Adv Polym Technol 2012;32:474–85. https://doi.org/10.1002/adv.

[90] Li L, Raasch TW, Yi AY. Simulation and measurement of optical aberrations of injection molded progressive addition lenses. Appl Opt 2013;52:6022–9. https://doi.org/10.1364/AO.52.006022.

[91] Isayev AI, Lin TH, Kwon K. Frozen-in birefringence and anisotropic shrinkage in optical moldings: II. Comparison of simulations with experiments on light-guide plates. Polymer 2010;51:5623–39. https://doi.org/10.1016/j.polymer.2010.09.055.

[92] Zhu J, Chen Y, Huang W, Zhang Q, Liao X, Huang Y, et al. Effect of injection compression process parameters on residual stress of products based on numerical simulation. J Phys Conf Ser 2019;1187:032031. https://doi.org/10.1088/1742-6596/1187/3/032031.

[93] Lin C, Tan C, Wang C. Gate design optimization in the injection molding of the optical lens. Optoelectron Adv Mater - Rapid Commun 2013;7:580–4.

[94] Bu Q, Zhu J, Yin Q. Injection compression molding process and mould design of plastic optical lens. Key Eng Mater 2012;501:321–4. 10.4028/www.scientific.net/KEM.501.321.

[95] Tsai KM, Lin YW. Quality improvement of optical lenses using innovative runner design. Int J Manuf Res 2013;8:337–56. https://doi.org/10.1504/IJMR.2013.057746.

[96] MacLeod HA. Thin-film optical filters. fourth ed. Arizona, USA: CRC Press, Taylor & Francis Group; 2018.

[97] Vahala KR. Optical microcavities. Nature 2003;424:839–46. https://doi.org/10.1038/nature01939.

[98] Notomi M, Kuramoch E, Taniyama H. Ultrahigh-Q nanocavity with 1D photonic gap. Opt Express 2008;16:11095–102. https://doi.org/10.1364/oe.16.011095.

[99] Xu X, Jin S. Strong coupling of single quantum dots with low-refractive-index/high-refractive-index materials at room temperature. Sci Adv 2020;6:eabb3095. https://doi.org/10.1126/sciadv.abb3095.

[100] Petasch W, Räiuchle E, Walker M, Eisner P. Improvement of the adhesion of low-energy polymers by a short-time plasma treatment. Surf Coating Technol 1995;74–75:682–8. https://doi.org/10.1016/0257-8972(94)08209-X.

[101] Hegemann D, Brunner H, Oehr C. Plasma treatment of polymers for surface and adhesion improvement. Nucl Instrum Methods Phys Res B 2003;208:281–6. https://doi.org/10.1016/s0168-583x(03)00644-x.

[102] Kupfer H, Wolf GK. Plasma and ion beam assisted metallization of polymers and their application. Nucl Instrum Methods Phys Res B-Beam Interact Mater Atoms 2000;166:722–31. https://doi.org/10.1016/s0168-583x(99)01192-1.

[103] Piegari A, Flory F. Optical thin films and coatings : from materials to applications. second ed. Cambridge, UK: Woodhead Publishing Limited; 2018.

[104] Raut HK, Ganesh VA, Nair AS, Ramakrishna S. Anti-reflective coatings: a critical, in-depth review. Energy Environ Sci 2011;45:3779–804. https://doi.org/10.1039/c1ee01297e.

[105] Brewis DM, Briggs D. Adhesion to polyethylene and polypropylene. Polymer 1981;22:7–16. https://doi.org/10.1016/0032-3861(81)90068-9.

[106] Kitanova S, Minchev M, Danev G. RF plasma treatment of polycarbonate substrates. J Optoelectron Adv Mater 2005;7:2607–12.

[107] Fujinami Y, Hayashi H, Ebe A, Imai O, Ogata K. Effect of sputtering-cleaning on adhesion of the metallic films to polymer substrates. Mater Chem Phys 1998;54:102–5. https://doi.org/10.1016/s0254-0584(98)00094-7.

[108] Peeling J, Clark DT. Surface ozonation and photooxidation of polyethylene film. J Polym Sci Polym Chem Ed 1983;21:2047–55. https://doi.org/10.1002/pol.1983.170210715.

[109] Hamdi M, Poulis JA. Effect of UV/ozone treatment on the wettability and adhesion of polymeric systems. J Adhes 2019;97:651–71. https://doi.org/10.1080/00218464.2019.1693372.

[110] Grundke K, Pöschel K, Synytska A, Frenzel R, Drechsler A, Nitschke M, et al. Experimental studies of contact angle hysteresis phenomena on polymer surfaces — toward the understanding and control of wettability for different applications. Adv Colloid Interface Sci 2015;222:350–76.

[111] Awaja F, Gilbert M, Kelly G, Fox B, Pigram PJ. Adhesion of polymers. Prog Polym Sci 2009;34:948–68. https://doi.org/10.1016/j.progpolymsci.2009.04.007.

[112] Brostow W, Lobland H, Hnatchuk N, Perez J. Improvement of scratch and wear resistance of polymers by fillers including nanofillers. Nanomaterials 2017;7:66. https://doi.org/10.3390/nano7030066.

[113] Mattaparthi S, Sharma CS. Fabrication of self-cleaning antireflective polymer surfaces by mimicking underside leaf hierarchical surface structures. J Bionic Eng 2019;16:400–9.

[114] Xu LKRG, Guo J, Yang S. Transparent, superhydrophobic surfaces from one-step spin coating of hydrophobic nanoparticles. ACS Appl Mater Interfaces 2012;4:1118–25. https://doi.org/10.1021/am201750h.

[115] Latthe S, Liu S, Terashima C, Nakata K, Fujishima A. Transparent, adherent, and photocatalytic sio2-tio2 coatings on polycarbonate for self-cleaning applications. Coatings 2014;4:497–507.

[116] Fateh R, Dillert R, Bahnemann D. Preparation and characterization of transparent hydrophilic photocatalytic tio2/sio2 thin films on polycarbonate. Langmuir 2013;29:3730–9. https://doi.org/10.1021/la400191x.

[117] Mavukkandy MO, McBride SA, Warsinger DM, Dizge N, Hasan SW, Arafat HA. Thin film deposition techniques for polymeric membranes– A review. J Membr Sci 2020;610:1–26. https://doi.org/10.1016/j.memsci.2020.118258.

[118] Schulz U. Review of modern techniques to generate antireflective properties on thermoplastic polymers. Appl Opt 2006;45:1608–18. https://doi.org/10.1364/ao.45.001608.

[119] Kuhr M, Bauer S, Rothhaar U, Wolff D. Coatings on plastics with the PICVD technology. Thin Solid Films 2003;442:107–16. https://doi.org/10.1016/s0040-6090(03)00956-8.

[120] Walheim S, Schaffer E, Mlynek J, Steiner U. Nanophase-separated polymer films as high-performance antireflection coatings. Science 1999;283:520–2. https://doi.org/10.1126/science.283.5401.520.

[121] Oliveira PW, Krug H, Frantzen A, Mennig M, Schmidt H. Generation of wet-chemical AR-coatings on plastic substrates by use of polymerizable nanoparticles. Sol-Gel Opt Iv 1997;3136:452–61. https://doi.org/10.1117/12.284139.

[122] Yoldas BE. Polymerized soluction for depositing optical oxide coatings. In: United States Patent. US 4,346,131; 1982.

[123] Ye LQ, Zhang YL, Zhang XX, Hu T, Ji R, Ding B, et al. Sol-gel preparation of SiO2/TiO2/SiO2-TiO2 broadband antireflective coating for solar cell cover glass. Sol Energy Mater Sol Cells 2013;111:160–4. https://doi.org/10.1016/j.solmat.2012.12.037.

[124] Felton LA. Characterization of coating systems. AAPS PharmSciTech 2007;8:E112. https://doi.org/10.1208/pt0804112.

[125] Dimitriou MD, Kramer Edward J, Hawker Craig J. Advanced techniques for the characterization of surface structure in polymer thin films and coatings. Arabian J Sci Eng 2014;39:1–13. https://doi.org/10.1007/S13369-013-0916-3.

[126] Tkadletz M, Schalk N, Daniel R, Keckes J, Czettl C, Mitterer C. Advanced characterization methods for wear resistant hard coatings: a review on recent progress. Surf Coating Technol 2016;285:31–46. https://doi.org/10.1016/j.surfcoat.2015.11.016.

[127] Kaliyannan GV, Palanisamy SV, Priyanka E, Thangavel S, Sivaraj S, Rathanasamy R. Investigation on sol-gel based coatings application in energy

sector – a review. Mater Today Proc 2021;45:1138–43. https://doi.org/10.1016/j.matpr.2020.03.484.
[128] Shanmugam N, Pugazhendhi R, Elavarasan RM, Kasiviswanathan P, Das N. Anti-reflective coating materials: a holistic review from PV perspective. Energies 2020;13:2631. https://doi.org/10.3390/en13102631.
[129] Rajan G, Karki S, Collins RW, Podraza NJ, Marsillac S. Real-time optimization of anti-reflective coatings for CIGS solar cells. Materials 2020;13:4259. https://doi.org/10.3390/ma13194259.
[130] Kumar V, Guleria P, Dasgupta N, Ranjan S. Functionalized nanomaterials II: applications. first ed. Boca Raton: CRC Press; 2021. https://doi.org/10.1201/9781351021388.
[131] Sirohi RS. Introduction to optical metrology. CRC Press, Taylor & Francis Group; 2016.
[132] Malkiat S. Johal. Intermolecular interactions and self- assembly. Understanding nanomaterials. 1º. CRC Press; 2012. p. 29–74. https://doi.org/10.1201/b11545.
[133] Tofteberg T, Amédro H, Andreassen E. Injection molding of a diffractive optical element. Polym Eng Sci 2008;48:2134–42. https://doi.org/10.1002/pen.21154.
[134] Loaldi D, Regi F, Baruffi F, Calaon M, Quagliotti D, Zhang Y, et al. Experimental validation of injection molding simulations of 3D microparts and microstructured components using virtual design of experiments and multi-scale modeling. Micromachines 2020;11:1–17. https://doi.org/10.3390/mi11060614.
[135] Zhang H, Zhang N, Han W, Gilchrist MD, Fang F. Precision replication of microlens arrays using variotherm-assisted microinjection moulding. Precis Eng 2021;67:248–61. https://doi.org/10.1016/j.precisioneng.2020.09.026.
[136] Lee BK, Kim DS, Kwon TH. Replication of microlens arrays by injection molding. Microsyst Technol 2004;10:531–5. https://doi.org/10.1007/s00542-004-0387-2.
[137] Hansen HN, Hocken RJ, Tosello G. Replication of micro and nano surface geometries. CIRP Ann - Manuf Technol 2011;60:695–714. https://doi.org/10.1016/j.cirp.2011.05.008.
[138] Kuo CC, Chen BC. Optimization of hot embossing molding process parameters of Fresnel lens using Taguchi method. Mater Werkst 2015;46:942–8. https://doi.org/10.1002/mawe.201500443.
[139] Worgull M, Schneider M, Heilig M, Kolew A, Dinglreiter H, Mohr J. Replication of optical components by hot embossing. Micro-Optics 2010:7716. https://doi.org/10.1117/12.859077.
[140] Heckele M, Bacher W, Hanemann T, Ulrich H. Hot embossing and injection molding for microoptical components. Proc SPIE-Int Soc Opt Eng 2013;3135:24–9. https://doi.org/10.1117/12.284110.
[141] He Y, Fu JZ, Chen ZC. Research on optimization of the hot embossing process. J Micromech Microeng 2007;17:2420–5. https://doi.org/10.1088/0960-1317/17/12/005.
[142] Becker H, Heim U. Hot embossing as a method for the fabrication of polymer high aspect ratio structures. Sens Actuat A Phys 2000;83:130–5. https://doi.org/10.1016/S0924-4247(00)00296-X.
[143] Shen YK, Chang CY, Shen YS, Hsu SC, Wu MW. Analysis for microstructure of microlens arrays on micro-injection molding by numerical simulation. Int Commun Heat Mass Tran 2008;35:723–7. https://doi.org/10.1016/j.icheatmasstransfer.2008.01.013.
[144] Rosato D, Rosato DV, Rosato MG. Specialized injection molding processes. Inject. Molding Handb. third ed. Norwell: Kluwer Academic Publishers; 2000. p. 1197–269.
[145] Baruffi F, Charalambis A, Calaon M, Elsborg R, Tosello G. Comparison of micro and conventional injection moulding based on process precision and accuracy. Procedia CIRP 2018;75:149–54. https://doi.org/10.1016/j.procir.2018.04.046.
[146] Muanchan P, Kaneda R, Ito H. Polymer materials structure and properties in micro injection molding parts. In: Tosello G, editor. Micro Inject. Molding. first ed. Munich: Hanser Gardner Publications; 2018. p. 57–81.
[147] Giboz J, Copponnex T, Patrice M. Microinjection molding of thermoplastic polymers : a review. J Micromech Microeng 2007;17:R96–109. https://doi.org/10.1088/0960-1317/17/6/R02.
[148] Masato D, Sorgato M, Lucchetta G. Characterization of the micro injection-compression molding process for the replication of high aspect ratio micro-structured surfaces. Microsyst Technol 2017;23:3661–70. https://doi.org/10.1007/s00542-016-3149-z.
[149] Metwally K, Barriere T, Khan-Malek C. Replication of micrometric and sub-micrometric structured surfaces using micro-injection and micro-injection compression moulding. Int J Adv Manuf Technol 2016;83:779–89. https://doi.org/10.1007/s00170-015-7602-4.
[150] Zhang H, Fang F, Gilchrist MD, Zhang N. Filling of high aspect ratio micro features of a microfluidic flow cytometer chip using micro injection moulding. J Micromech Microeng 2018;28:075005. https://doi.org/10.1088/1361-6439/aab7bf.
[151] Zhang N, Chu JS, Byrne CJ, Browne DJ, Gilchrist MD. Replication of micro/nano-scale features by micro injection molding with a bulk metallic glass mold insert. J Micromech Microeng 2012;22:1–13. https://doi.org/10.1088/0960-1317/22/6/065019.
[152] Sha B, Dimov S, Griffiths C, Packianather MS. Investigation of micro-injection moulding: factors affecting the replication quality. J Mater Process Technol 2007;183:284–96. https://doi.org/10.1016/j.jmatprotec.2006.10.019.
[153] Theilade UA, Hansen HN. Surface microstructure replication in injection molding. Int J Adv Manuf Technol 2007;33:157–66. https://doi.org/10.1007/s00170-006-0732-y.
[154] Maghsoudi K, Jafari R, Momen G, Farzaneh M. Micro-nanostructured polymer surfaces using injection molding: a review. Mater Today Commun 2017;13:126–43. https://doi.org/10.1016/j.mtcomm.2017.09.013.
[155] Yang C, Huang H-X, Castro J, Yi A. Replication characterization in injection molding of microfeatures with high aspect ratio: influence of layout and shape factor. Polym Eng Sci 2011;51:959–68. https://doi.org/10.1002/pen.21914.
[156] Liparoti S, Calaon M, Speranza V, Tosello G, Pantani R, Hansen NH, et al. Effects of fast mold temperature evolution on micro features replication quality during injection molding. AIP conference Proceedings, vol. 1914. AIP Publishing; 2017. https://doi.org/10.1063/1.5016772. 140007–1.
[157] Baruffi F, Calaon M, Tosello G. Effects of micro-injection moulding process parameters on accuracy and precision of thermoplastic elastomer micro rings. Precis Eng 2018;51:353–61. https://doi.org/10.1016/j.precisioneng.2017.09.006.
[158] Piccolo L, Sorgato M, Batal A, Dimov S, Lucchetta G, Masato D. Functionalization of plastic parts by replication of variable pitch laser-induced periodic surface structures. Micromachines 2020;11. https://doi.org/10.3390/MI11040429.
[159] Masato D, Sorgato M, Lucchetta G. Analysis of the influence of part thickness on the replication of micro-structured surfaces by injection molding. Mater Des 2016;95:219–24. https://doi.org/10.1016/j.matdes.2016.01.115.
[160] Lucchetta G, Sorgato M, Carmignato S, Savio E. Investigating the technological limits of micro-injection molding in replicating high aspect ratio micro-structured surfaces. CIRP Ann - Manuf Technol 2014;63:521–4. https://doi.org/10.1016/j.cirp.2014.03.049.
[161] Chen L, Kirchberg S, Jiang BY, Xie L, Jia YL, Sun LL. Fabrication of long-focal-length plano-convex microlens array by combining the micro-milling and injection molding processes. Appl Opt 2014;53:7369–80. https://doi.org/10.1364/AO.53.007369.
[162] Sorgato M, Lucchetta G. The evaluation of vacuum venting and variotherm process for improving the replication by injection molding of high aspect ratio micro features for biomedical application. AIP Conf Proc 2015;1664:1–5. https://doi.org/10.1063/1.4918483.
[163] Sorgato M, Babenko M, Lucchetta G, Whiteside B. Investigation of the influence of vacuum venting on mould surface temperature in micro injection moulding. Int J Adv Manuf Technol 2017;88:547–55. https://doi.org/10.1007/s00170-016-8789-8.
[164] Park SH, Lee WI, Moon SN, Yoo YE, Cho YH. Injection molding micro patterns with high aspect ratio using a polymeric flexible stamper. Express Polym Lett 2011;5:950–8. https://doi.org/10.3144/expresspolymlett.2011.93.
[165] Rohde M, Derdouri A, Kamal MR. Micro replication by injection-compression molding. Int Polym Process 2009;24:288–97. https://doi.org/10.3139/217.2264.
[166] Huang M-S, Chung C-F. Injection molding and injection compression moldingof thin-walled light-guided plates with V-GroovedMicrofeatures. J Appl Polym Sci 2011;121:1151–9. https://doi.org/10.1002/app.
[167] Roeder M, Thiele S, Hera D, Pruss C, Guenther T, Osten W, et al. Fabrication of curved diffractive optical elements by means of laser direct writing, electroplating, and injection compression molding. J Manuf Process 2019;47:402–9. https://doi.org/10.1016/j.jmapro.2019.10.012.
[168] Bernhard CG, Miller WH. A corneal nipple pattern in insect compound eyes. Acta Physiol Scand 1962;56:385. https://doi.org/10.1111/j.1748-1716.1962.tb02515.x.
[169] Jang HJ, Kim YJ, Yoo YJ, Lee GJ, Kim MS, Chang KS, et al. Double-sided anti-reflection nanostructures on optical convex lenses for imaging applications. Coatings 2019;9:1–8. https://doi.org/10.3390/coatings9060404.
[170] Han Z, Wang Z, Li B, Feng X, Jiao Z, Zhang J, et al. Flexible self-cleaning broadband Antireflective film inspired by the transparent cicada wings. ACS Appl Mater Interfaces 2019;11:17019–27. https://doi.org/10.1021/acsami.9b01948.
[171] Li Z, Song C, Li Q, Xiang X, Yang H, Wang X, et al. Hybrid nanostructured antireflection coating by self-assembled nanosphere lithography. Coatings 2019;9:1–10. https://doi.org/10.3390/coatings9070453.
[172] Cai J, Qi L. Recent advances in antireflective surfaces based on nanostructure arrays. Mater Horizons 2015;2:37–53. https://doi.org/10.1039/C4MH00140K.
[173] Xie SP, Wan XJ, Yang B, Zhang W, Wei XX, Zhuang SL. Design and fabrication of wafer-level microlens array with moth-eye antireflective nanostructures. Nanomaterials 2019;9. https://doi.org/10.3390/nano9050747.
[174] Jacobo-Martin A, Rueda M, Hernandez JJ, Navarro-Baena I, Monclus MA, Molina-Aldareguia JM, et al. Bioinspired antireflective flexible films with optimized mechanical resistance fabricated by roll to roll thermal nanoimprint. Sci Rep 2021;11:1–15. https://doi.org/10.1038/s41598-021-81560-6.
[175] Tan G, Lee J-H, Lan Y-H, Wei M-K, Peng L-H, Cheng I-C, et al. Broadband antireflection film with moth-eye-like structure for flexible display applications. Optica 2017;4:678–83. https://doi.org/10.1364/OPTICA.4.000678.
[176] Prajapati A, Llobet J, Antunes M, Martins S, Fonseca H, Calaza C, et al. Opportunities for enhanced omnidirectional broadband absorption of the solar radiation using deep subwavelength structures. Nano Energy 2020;70:104553. https://doi.org/10.1016/j.nanoen.2020.104553.
[177] Fernandez A, Francone A, Thamdrup LH, Johansson A, Bilenberg B, Nielsen T, et al. Hierarchical surfaces for enhanced self-cleaning applications. J Micromech Microeng 2017;27. https://doi.org/10.1088/1361-6439/aa62bb.
[178] Pattantyus-Abraham A, Krahn J, Menon C. Recent advances in nanostructured biomimetic dry adhesives. Front Bioeng Biotechnol 2013;1:1–10. https://doi.org/10.3389/fbioe.2013.00022.
[179] Sun J, Wang X, Wu J, Jiang C, Shen J, Cooper MA, et al. Biomimetic moth-eye nanofabrication: enhanced antireflection with superior self-cleaning characteristic. Sci Rep 2018;8:1–10. https://doi.org/10.1038/s41598-018-23771-y.
[180] Roeder M, Guenther T, Zimmermann A. Review on fabrication technologies for optical mold inserts. Micromachines 2019;10:1–25. https://doi.org/10.3390/mi10040233.

[181] Kwon B, Kim JH. Importance of molds for nanoimprint lithography: hard, soft, and hybrid molds. J Nanosci 2016:1–12. https://doi.org/10.1155/2016/6571297.
[182] Kim DS, Lee HS, Lee B-K, Yang SS, Kwon TH, Lee SS. Replications and analysis of microlens array fabricated by a modified LIGA process. Polym Eng Sci 2006;46:416–25. https://doi.org/10.1002/pen.
[183] Moon S, Lee N, Kang S. Fabrication of a microlens array using micro-compression molding with an electroformed mold insert. J Micromech Microeng 2002;13:98–103. https://doi.org/10.1088/0960-1317/13/1/314.
[184] Zolfaghari A, Zhang L, Zhou W, Yi AY. Replication of plastic microlens arrays using electroforming and precision compression molding. Microelectron Eng 2021;239–240:111529. https://doi.org/10.1016/j.mee.2021.111529.
[185] Huang C, Li L, Yi AY. Design and fabrication of a micro Alvarez lens array with a variable focal length. Microsyst Technol 2009;15:559–63. https://doi.org/10.1007/s00542-008-0706-0.
[186] Yi A, Li L. Design and fabrication of a microlens array by use of a slow tool servo. Opt Lett 2005;30:1707–9. https://doi.org/10.1364/ol.30.001707. PMID: 16075545.
[187] Zhang X, Fang F, Yu L, Jiang L, Guo Y. Slow slide servo turning of compound eye lens. Opt Eng 2013;52:023401. https://doi.org/10.1117/1.oe.52.2.023401.
[188] Klocke F, Dambon O, Bulla B. Diamond turning of aspheric steel molds for optics replication. Proc SPIE-Int Soc Opt Eng 2010;7590. https://doi.org/10.1117/12.839422.
[189] Sweatt WC, Gill DD, Adams DP, Vasile MJ, Claudet AA. Diamond milling of micro-optics. IEEE Aero Electron Syst Mag 2008;23:13–7. https://doi.org/10.1109/AES-M.2008.4444483.
[190] Takino H, Hosaka T. Shaping of steel mold surface of lens array by electrical discharge machining with single rod electrode. Appl Opt 2014;53. https://doi.org/10.1364/AO.53.008002. 8002–5.
[191] Yanagishita T, Hidaka T, Suzuki M, Masuda H. Polymer lenses with antireflection structures prepared using anodic porous alumina molds. J Vac Sci Technol B 2016;34:021804. https://doi.org/10.1116/1.4943044.
[192] Roeder M, Schilling P, Fritz KP, Guenther T, Zimmermann A. Challenges in the fabrication of microstructured polymer optics. J Micro Nano-Manufacturing 2019;7. https://doi.org/10.1115/1.4044219.
[193] Lantada AD, Pfleging W, Besser H, Guttmann M, Wissmann M, Plewa K, et al. Research on the methods for the mass production of multi-scale organs-on-chips. Polymers 2018;10:1–17. https://doi.org/10.3390/polym10111238.
[194] Masato D, Sorgato M, Lucchetta G. Analysis of the influence of part thickness on the replication of micro-structured surfaces by injection molding. Mater Des 2016;95:219–24. https://doi.org/10.1016/j.matdes.2016.01.115.
[195] Mielonen K, Pakkanen TA. Superhydrophobic hierarchical three-level structures on 3D polypropylene surfaces. J Micromech Microeng 2019;29. https://doi.org/10.1088/1361-6439/aaf7e4.
[196] Bellantone V, Surace R, Modica F, Fassi I. Evaluation of mold roughness influence on injected thin micro-cavities. Int J Adv Manuf Technol 2018;94:4565–75. https://doi.org/10.1007/s00170-017-1178-0.
[197] Sorgato M, Masato D, Lucchetta G. Effect of vacuum venting and mold wettability on the replication of micro-structured surfaces. Microsyst Technol 2017;23:2543–52. https://doi.org/10.1007/s00542-016-3038-5.
[198] Chen SC, Jong WR, Chang YJ, Chang JA, Cin JC. Rapid mold temperature variation for assisting the micro injection of high aspect ratio micro-feature parts using induction heating technology. J Micromech Microeng 2006;16:1783–91. https://doi.org/10.1088/0960-1317/16/9/005.
[199] Rytka C, Kristiansen PM, Neyer A. Iso- and variothermal injection compression moulding of polymer micro- and nanostructures for optical and medical applications. J Micromech Microeng 2015;25. https://doi.org/10.1088/0960-1317/25/6/065008.
[200] Xie L, Ziegmann G. A visual mold with variotherm system for weld line study in micro injection molding. Microsyst Technol 2008;14:809–14. https://doi.org/10.1007/s00542-008-0566-7.
[201] Wang G long, Zhao G qun, Wang X xin. Heating/cooling channels design for an automotive interior part and its evaluation in rapid heat cycle molding. Mater Des 2014;59:310–22. https://doi.org/10.1016/j.matdes.2014.02.047.
[202] Zhang N, Zhang H, Stief P, Dantan J, Etienne A, Siadat A. Geometric replication integrity of micro features fabricated using variotherm assisted micro injection moulding. Procedia CIRP 2018;71:390–5. https://doi.org/10.1016/j.procir.2018.05.049.
[203] Yu MC, Young W Bin, Hsu PM. Micro-injection molding with the infrared assisted mold heating system. Mater Sci Eng A 2007;460–461:288–95. https://doi.org/10.1016/j.msea.2007.02.036.
[204] Su Q, Zhang N, Gilchrist MD. The use of variotherm systems for microinjection molding. J Appl Polym 2016;42962:1–17. https://doi.org/10.1002/app.42962.
[205] Zhang N, Zhang H, Stallard C, Fang F, Gilchrist MD. Replication integrity of micro features using variotherm and vacuum assisted microinjection moulding. CIRP J Manuf Sci Technol 2018;23:20–38. https://doi.org/10.1016/j.cirpj.2018.10.002.
[206] Lin HL, Chen SC, Jeng MC, Minh PS, Chang JA, Hwang JR. Induction heating with the ring effect for injection molding plates. Int Commun Heat Mass Tran 2012;39:514–22. https://doi.org/10.1016/j.icheatmasstransfer.2012.02.009.
[207] Chen S-C, Lin S-H, Minh PS, Chang J-A, Huang S-W. Dynamic mold temperature control using external wrapped inductor heating combined with coolant cooling. Seikei-Kakou 2012;24:477–81. https://doi.org/10.4325/seikeikakou.24.477.
[208] Wang G, Zhao G, Li H, Guan Y. Research of thermal response simulation and mold structure optimization for rapid heat cycle molding processes, respectively, with steam heating and electric heating. Mater Des 2010;31:382–95. https://doi.org/10.1016/j.matdes.2009.06.010.
[209] Wang M, Dong J, Wang W, Zhou J, Dai Z, Zhuang X, et al. Optimal design of medium channels for water-assisted rapid thermal cycle mold using multi-objective evolutionary algorithm and multi-attribute decision-making method. Int J Adv Manuf Technol 2013;68:2407–17. https://doi.org/10.1007/s00170-013-4868-2.
[210] Jeng MC, Chen SC, Minh PS, Chang JA, Chung C shen. Rapid mold temperature control in injection molding by using steam heating. Int Commun Heat Mass Tran 2010;37:1295–304. https://doi.org/10.1016/j.icheatmasstransfer.2010.07.012.
[211] Sánchez R, Martinez A, Mercado D, Carbonel A, Aisa J. Rapid heating injection moulding: an experimental surface temperature study. Polym Test 2020;93:106928. https://doi.org/10.1016/j.polymertesting.2020.106928.
[212] Chen SC, Chien R Der, Lin SH, Lin MC, Chang JA. Feasibility evaluation of gas-assisted heating for mold surface temperature control during injection molding process. Int Commun Heat Mass Tran 2009;36:806–12. https://doi.org/10.1016/j.icheatmasstransfer.2009.06.007.
[213] Chen M, Yao D, Kim B. Eliminating flow induced birefringence and minimizing thermally induced residual stresses in injection molded parts. Polym Plast Technol Eng 2001;40:491–503. https://doi.org/10.1081/PPT-100002072.
[214] Park K, Kim B, Yao D. Numerical simulation for injection molding with a rapidly heated mold, Part II: birefringence prediction. Polym Plast Technol Eng 2006;45:903–9. https://doi.org/10.1080/03602550600718167.
[215] Hong S, Min I, Yoon K, Kang J. Effects of adding injection-compression to rapid heat cycle molding on the structure of a light guide plate. J Micromech Microeng 2014;24. https://doi.org/10.1088/0960-1317/24/1/015009.
[216] Lucchetta G, Fiorotto M, Bariani PF. Influence of rapid mold temperature variation on surface topography replication and appearance of injection-molded parts. CIRP Ann - Manuf Technol 2012;61:539–42. https://doi.org/10.1016/j.cirp.2012.03.091.
[217] Chen SC, Chang JA, Hsu WY, Huang SW. Improvement of replication accuracy of micro-featured molding using gas-assisted heating for mold surface. Microelectron Eng 2011;88:1594–600. https://doi.org/10.1016/j.mee.2011.02.055.
[218] Lan X, Li C, Yang C, Xue C. Optimization of injection molding process parameters and axial surface compensation for producing an aspheric plastic lens with large diameter and center thickness. Appl Opt 2019;58:927–34. https://doi.org/10.1364/AO.58.000927.
[219] Park H, Cha BS, Choi KI, Chang HK, Rhee B. Manufacturing of thick-wall plastic lens mold with conformal cooling channel using rapid tooling technology. J KSDME 2007;1:1181–6.
[220] Khan M, Afaq SK, Khan NU, Ahmad S. Cycle time reduction in injection molding process by selection of robust cooling channel design. ISRN Mech Eng 2014:1–8. https://doi.org/10.1155/2014/968484Research.
[221] Dimla DE, Camilotto M, Miani F. Design and optimisation of conformal cooling channels in injection moulding tools. J Mater Process Technol 2005;164–165:1294–300. https://doi.org/10.1016/j.jmatprotec.2005.02.162.
[222] Kitayama S, Miyakawa H, Takano M, Aiba S. Multi-objective optimization of injection molding process parameters for short cycle time and warpage reduction using conformal cooling channel. Int J Adv Manuf Technol 2017;88:1735–44. https://doi.org/10.1007/s00170-016-8904-x.
[223] Tan C, Wang D, Ma W, Chen Y, Chen S, Yang Y, et al. Design and additive manufacturing of novel conformal cooling molds. Mater Des 2020;196:109147. https://doi.org/10.1016/j.matdes.2020.109147.
[224] Kitchloo P, Payne N, Tisne S. System and method for conformal cooling during a lens manufacturing process. In: United States Patent. US 2019/0111588 A1; 2019.
[225] Chung CY. Integrated optimum layout of conformal cooling channels and optimal injection molding process parameters for optical lenses. Appl Sci 2019;9. https://doi.org/10.3390/app9204341.